Biomass and Bioenergy 146 (2021) 105975

Contents lists available at ScienceDirect

Biomass and Bioenergy

journal homepage: http://www.elsevier.com/locate/biombioe

SunnGro: A new crop model for the simulation of sunn hemp (*Crotalaria juncea* L.) grown under alternative management practices

Andrea Parenti [a,*], Giovanni Cappelli [b], Walter Zegada-Lizarazu [a], Carlos Martín Sastre [c], Myrsini Christou [d], Andrea Monti [a], Fabrizio Ginaldi [b]

[a] DISTAL – Department of Agricultural and Food Sciences, University of Bologna, Viale G. Fanin 44, 40127, Bologna, Italy
[b] CREA – Council for Agricultural Research and Economics, Research Centre for Agriculture and Environment, via di Corticella 133, 40128, Bologna, Italy
[c] CIEMAT – Research Centre for Energy, Environment and Technology, CEDER, Autovía de Navarra A15, S56, 42290, Lubia, Soria, Spain
[d] CRES – Center for Renewable Energy Sources and Saving, 19th km Marathonos Ave., 19009, Pikermi, Greece

ARTICLE INFO

Keywords:
Advanced biofuel
BioMA modeling platform
Bioenergy crop
Crop rotation
Crop intensification
Double crop
Legume

ABSTRACT

Sunn hemp (*Crotalaria juncea* L.) is a fast growing, drought tolerant legume crop with potential as a biomass feedstock for advanced biofuels in Southern Europe, grown in either a single or double crop system. This study presents a new simulation model, SunnGro, which reproduces sunn hemp productivity, while providing a detailed description of leaf/branch size heterogeneity and its evolution during the vegetative season. The model was calibrated and validated using 20 field datasets collected from 2016 to 2018 in Greece, Spain, and Italy under non-limiting soil water conditions. High correlation between the simulated and measured values of branch number ($R^2 = 0.80$), leaf number ($R^2 = 0.92$), and biomass accumulation ($0.67 < R^2 < 0.82$) demonstrated good model predictivity across sites, seasons, alternative sowing densities, dates, and harvest times. An uncertainty analysis was carried out under varying seasonal air temperatures and sowing times in five European locations to explore the capability of the model to identify the best agronomic practices for maximizing sunn hemp yield. Therefore, the current version of SunnGro is an effective tool for scenario analyses under varying management practices and changing climatic conditions.

1. Introduction

Fallowing remains a common practice in conventional crop rotation in Southern Europe. Crop intensification can prevent soil erosion, reduce chemical treatments, and increase the multifunctionality of the agricultural sector [1]. On this basis, the BECOOL project (https://www.becoolproject.eu/) was launched to evaluate the biomass production potential in rotation systems at the European level, through the introduction of dedicated lignocellulosic crops for advanced biofuels within existing food/feed cropping systems. The identification of low input annual summer legumes, having the ability to grow as double crops (i.e., no competition with food crops), would be beneficial in terms of biodiversity, soil fertility, agroecological transition for sustainable agriculture [2], and feedstock diversification for the bioenergy sector [3]. Among warm-season legumes, sunn hemp (*Crotalaria juncea* L.) stands out in terms of biomass productivity compared to cowpea [4], pigeonpea [5], and other tropical legumes [6].

Sunn hemp is a fast-growing, C3 drought-tolerant legume crop [7] of tropical origin that is suited for growth in a wide range of soils [8,9] and is resistant to root-knot and soybean cyst nematodes [10]. It has widespread use in tropical areas as a source of bast fiber and green manure [11,12]. Canopy architecture is strongly affected by the emergence rate, plant density, and apical dominance, which in turn regulates leaf/-branch size heterogeneity and number, thus influencing the quantity and quality of the biomass at harvest [13,14]. When cultivated as a no-tillage double crop, i.e., after wheat, sunn hemp productivity does not decrease compared to conventional tillage management (around 7 Mg ha^{-1} in 90 days), with benefits in terms of time- and cost-saving management of crop operations [15]. Therefore, sunn hemp can be considered a promising summer crop with great potential as feedstock for advanced biofuels [16], particularly in multifunctional agricultural systems [17]. Cantrell et al. [18] obtained an average yield of 11 Mg ha^{-1} of dry biomass in a field experiment conducted in Florence (USA), which led to an energy yield of approximately 200 GJ ha^{-1} by considering a higher heating value of 19 MJ kg^{-1} (dw).

To date, sunn hemp productivity in humid subtropical environments has been poorly investigated [12,19], and information is even scarcer for

* Corresponding author.
E-mail address: andrea.parenti5@unibo.it (A. Parenti).

https://doi.org/10.1016/j.biombioe.2021.105975
Received 7 August 2020; Received in revised form 16 December 2020; Accepted 17 January 2021
Available online 9 February 2021

List of acronyms and abbreviations

AGB	aboveground biomass
avg	average
b, k	steepness coefficients
BECOOL	Brazil-EU Cooperation for Development of Advanced Lignocellulosic Biofuels
BioMA	Biophysical Model Application platform
BN	branch number
Cfa	hot-summer Mediterranean climate
Cfb	humid subtropical climate
CRM	coefficient of residual mass
Csa	marine west coast climate
DOY	day of the year
EF	modeling efficiency
em	emergence
GDD	growing degree day
HT	harvest time
ID	experimental number
IQD	interquartile distance
KGT	Köppen-Giger taxonomy
LL	leaf length
LN	leaves number
LW	leaf width
pbp	peak of branch population
PD	plant density
PH	phenology
SBN	secondary branch number
SD	sowing density
SDK	Software Development Kit
TPBN	time to reach peak branch number
TPLN	time to reach total number of leaves

temperate climates [15,20]. Hence, a comprehensive study on sunn hemp productivity under alternative management practices (sowing dates and density) in diverse European environments is yet to be performed.

Assessment of case-specific sunn hemp productivity via biophysical modeling represents a cost-effective solution to explore the crop potential response across different environments and under alternative management practices. Compared to model-based simulation experiments, *in vivo* multi-year and multi-site open-field trials are more expensive and time consuming, being mainly limited to a small number of experimental situations [21]. Biophysical models can fulfill these goals because of their ability to reproduce non-linear crop responses to variable pedo-climatic and management conditions [22]. Before local/large-scale models are applied, they are calibrated using reliable and representative sets of data for the conditions to be explored, i.e., model parameters are adjusted within their biophysical ranges to obtain an optimal agreement between the simulated and observed data. Examples of crop model applications in research studies involve the quantification of trade-offs among crop productivity, management, and the environment; assessment of climate change impacts on agricultural products; support of the implementation of adaptation strategies; impact of fungal diseases; and most recently, the evaluation of pre-harvest crop quality and design of future crop ideotypes [23]. Although a variety of generic (e.g., CROP-GRO [24], APSIM-Legume [25], and STICS [26]) and specific models [27–29] have been developed to simulate diverse legume species (e.g., common bean, peanut, soybean, cowpea, black gram, and chickpea), a process-based model of sunn hemp to investigate its biomass productivity potential is still lacking. The few prior modeling studies were all performed using a generic simulator, originally developed for cereals and adapted via parameterization (e.g., EPIC [30]), or using empirical relationships between productive/biometric traits (e.g., total dry matter, plant height, and stem diameters) and time after sowing [31,32].

Both generic process-based models and empirical approaches have intrinsic limitations. The former are limited because they do not explicitly consider the complex canopy architecture and heterogeneity typical of sunn hemp (e.g., non-homogeneous vegetation cover, plant branching, leaf area emission, and expansion). The latter are limited because they do not explain any relationship between agro-environmental conditions and crop growth and development. Therefore, the applicability of the available modeling approaches is limited to the conditions in which they were developed or calibrated. The integration of crop-specific empirical functions reproducing the development of sunn hemp canopy architecture into a biophysical process-based model for growth and development solves the above-mentioned issues and enables the representation of the system as a whole by dynamically simulating the interactions among sunn hemp productivity, weather, soil, and management practices.

Therefore, through a new user-friendly model application developed on a large dataset available either for public or private stakeholders, the assessment of sunn hemp potential would become a cost-effective operation for the development of advanced biofuels in Europe. To build a complete and reliable database for model calibration and validation, dedicated experimental field trials were performed under non-limiting conditions for water and nutrient availability (University of Bologna, UNIBO, for Italy; Research Centre for Energy, Environment and Technology, CIEMAT, for Spain; Centre for Renewable Energy Sources and Saving, CRES, for Greece), and subsequently, the collated datasets were shared with crop modeling partners (Council for Agricultural Research and Economics, CREA and UNIBO contribution).

The aim of the present study was to create a new process-based simulation model for sunn hemp, SunnGro, derived from the giant reed Arungro model [33], which in turn inherits about 70% of the code of the sugarcane DSSAT v4.5 CANEGRO model [34,35]. New algorithms reproducing branch and leaf size/number heterogeneity and their evolution over the growing season were developed and coded, and the resulting model was then calibrated and validated using field experiments carried out under alternative plant densities and harvesting times in Northern Italy, Spain, and Greece. It was then applied in a factorial experiment to assess its uncertainty in reproducing biomass accumulation under varying thermal conditions and sowing times/densities in five European locations suited for sunn hemp cultivation.

2. Materials and methods

A four-step workflow for this study is presented in Fig. 1.

The Arungro model [33] was used as the basis for the development of a new sunn hemp process-based model, SunnGro (*Step A,* section 2.2). Arungro, which provides a simulation of giant reed (*Arundo donax* L.) growth, is an extension of the Canegro model, from which it derives most of the algorithms connected to the simulation of phenology, leaf expansion, growth, and soil water balance. The main differences between the two models rely on the following: i) the formalization of tiller population dynamics (function of the development stage in Canegro and of rhizome biomass in Arungro); ii) the description of total and green leaf area index (LAI) dynamics (the maximum number of leaves on a tiller is indeterminate in Canegro and determinate in Arungro); iii) PAR interception (both models rely on the Lambert–Beer equation; however, in Arungro, the extinction coefficient is set at a constant value). We chose Arungro as our base because it already provided a detailed representation of the canopy structure and its dynamics over vegetative growth, compared to mono- and multi-layer crop models. Unlike

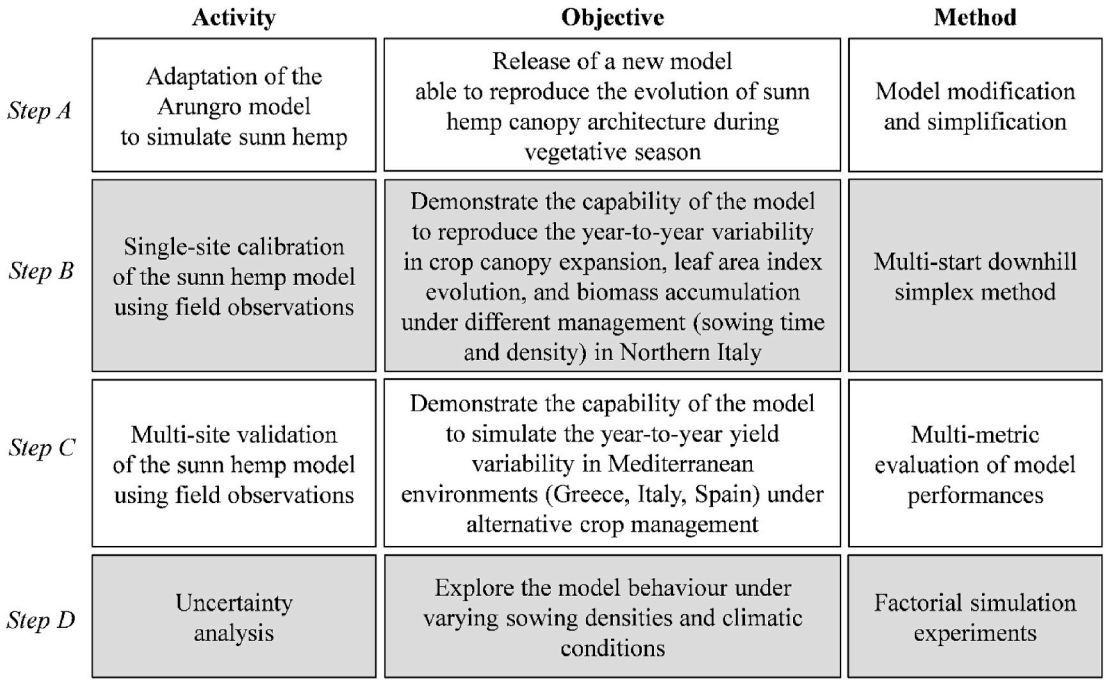

Fig. 1. Activities performed in the present study, with corresponding objectives and methodologies.

Arungro, SunnGro assumes that primary and secondary branches are representative of the whole stem population and replaces the original approaches for handling stem population, leaf number, and size evolution with species-specific algorithms. The simulation of the photosynthetic process, biomass accumulation, and partitioning of assimilates have been borrowed from the seminal model, although the number of model parameters was reduced.

A stepwise automatic calibration of the model was subsequently carried out using multi-year experimental data collected under different sowing times and densities in Northern-Italy (2016–2018), aimed at reproducing the dynamics of branch and leaf number, LAI ($m^2\ m^{-2}$), and aboveground biomass (AGB, Mg ha^{-1}) (*Step B*, section 2.3.1).

This activity laid the basis for a multi-site model validation (*Step C*, section 2.3.1), in which the calibrated parameter set was applied to reproduce AGB measurements from independent field trials carried out in three Mediterranean countries (Greece, Italy, and Spain).

Table 1
Datasets from Cadriano (Ca, Italy), Guadajira (G, Spain), and Aliartos (A, Greece) used for model calibration (C) and validation (V): phenology (PH), leaf number (LN, leaves $plant^{-1}$), leaf length (LL, mm), leaf width (LW, mm), branch number (BN, branches $plant^{-1}$), plant density (PD, plants m^{-2}), and aboveground biomass (AGB, Mg ha^{-1}). The overall number of samplings per variable is reported between brackets. Sowing d: sowing density; Tavg: average daily temperature during crop cycle; Reps n.: replications number; Rain: cumulative precipitation during crop cycle; Irr.: irrigation water.

ID	Site	Year	Sowing date	Harvest time	Sowing d (seed m^{-2})	Reps n.	Plot area (m^2)	Measured variables	Use	Tavg (°C)	Rain (mm)	Irr. (mm)
1	Ca	2016	18/05	1/08	52	1	64	PH(16), LN (26), BN(26), PD (10), AGB (8)	C	23.1	156	
2				23/08	104	1	64		C	23.5	196	
3					52	1	64		C			
4					33	1	70		C			
5				20/09	104	1	64		V	23.7	245	
6					52	1	64		V			
7					33	1	70		V			
8			22/06	25/10	52	1	64		V	22.9	220	
9	Ca	2017	26/06	10/10	52	4	135	PH(4), LN (18), LL (5), LW (5), BN(18), PD	C	24.2	182	174
10			5/07	26/10	52	4	231	(7), AGB (5), LAI (6)	C	24.1	167	201
11	Ca	2018	8/05	27/09	52	4	41	PH(6), LN (4), BN(4), PD (3), AGB (8), LAI	C	24.0	231	
12			25/05	9/10	52	4	231	(6)	C	24.2	221	16
13			2/07		52	4	231		C	24.5	161	
14	G	2018	1/06	8/10	52	4	120	AGB (2)	V	24.2	67	421
15	G		17/07	11/10	52	4	120		V	26.3	24	347
16	A	2017	21/05	27/10	13	3	13	PH(8), PD (4), AGB (4)	V	24.7	125	415
17					20	3	13		V			
18					40	3	13		V			
19			20/06		20	4	98		V	25.3	48	344
20	A	2018	16/06	1/10	20	4	98	PH(2), PD (1), AGB (1)	V	25.7	219	209

Finally, the model uncertainty to variations in mean seasonal air temperatures and sowing date (*Step D*, section 2.3.2) was assessed in five Southern and Eastern European locations suited for sunn hemp cultivation, using branch emission, leaf appearance, and AGB accumulation as target variables.

2.1. Field experiments used in model calibration and validation

2.1.1. Experimental design and agronomic management

During the 2016–2018 seasons (Appendix B, Fig. B1, B2, B3, and B.4, Table 1), the registered sunn hemp variety 'Ecofix' was tested in irrigated systems across the following three locations (Fig. 2): i) Cadriano, Italy (44° 33′ N, 32 m a.s.l.); ii) Guadajira, Spain (38° 51′ N, 222 m a.s.l.); iii) Aliartos, Greece (38° 22′ N, 114 m a.s.l.).

Thirteen samplings were performed in Italy over the 2016–2018 growing seasons. The soil was clay loam, with a neutral pH (6.6–7.4), rich in K_2O (~163 mg kg^{-1}), with average N and P_2O_5 contents of approximately 1.1 g kg^{-1} and 82 mg kg^{-1}, respectively, and 1.2% organic matter content. In 2017 and 2018, the experimental design was a randomized complete block (n = 4), while in 2016, an exploratory trial without replicates was conducted. A firm seedbed preparation was assured by two harrowings, and pre-sowing weed control was performed by glyphosate treatment (4 L ha^{-1}). Sunn hemp was sown with a pneumatic seeder alongside a granular soil sterilant application of lambda-cyhalothrin. The sowing density (SD) was 4.4 cm on the row, with three row spacings: 22.5 cm (high SD), 45 cm (medium SD), and 70 cm (low SD). The plots were kept weed-free by mechanical weeding when plant height reached around 30 cm. Fertilization was not applied due to the soil nutritional status (Appendix A, Table A1 in supplementary material), which was sufficient to meet the crop N-requirements, as demonstrated by Parenti et al. [36], in a dedicated study conducted on the same crop, field, and period. Sprinkler irrigation was performed in

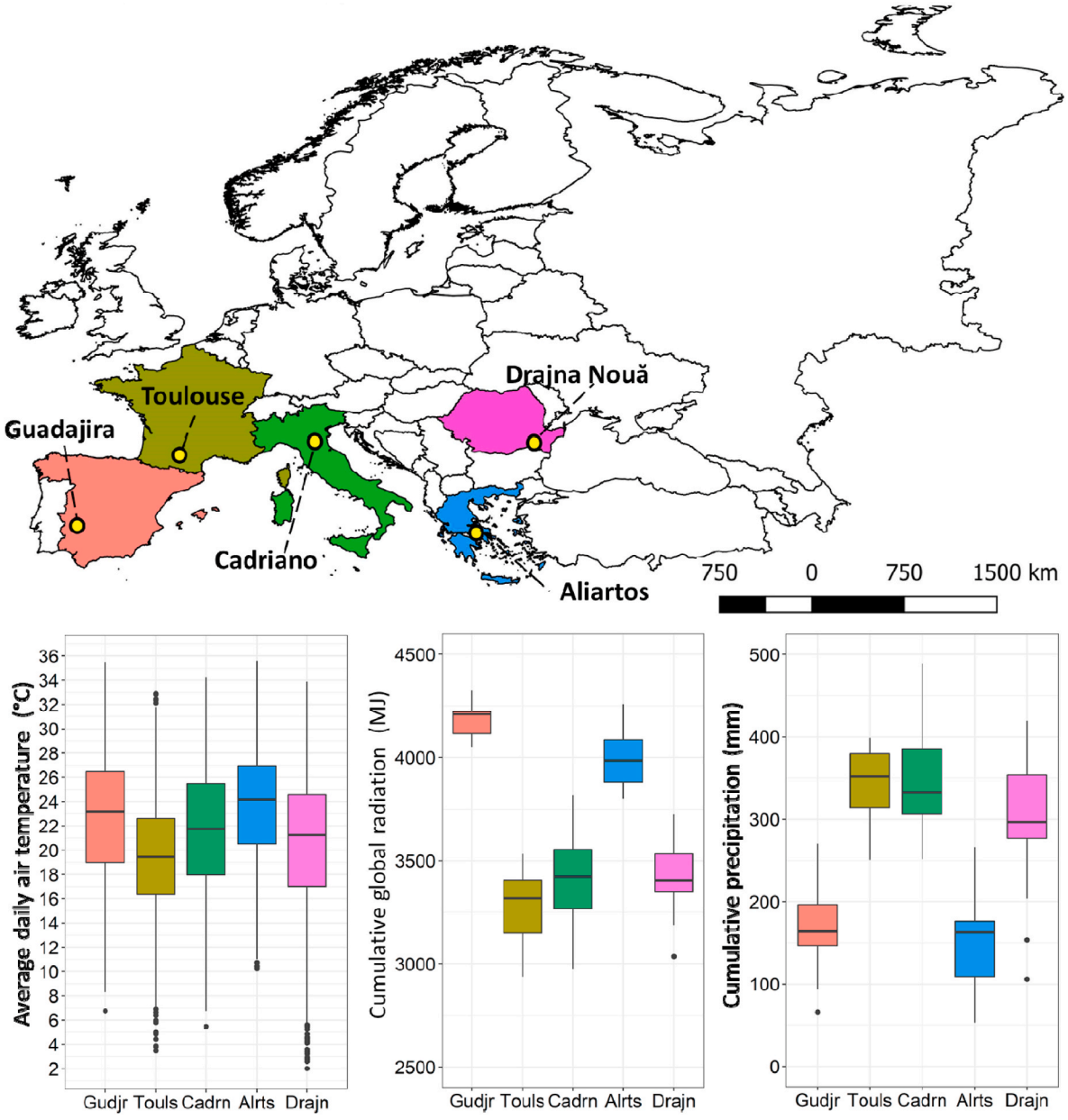

Fig. 2. Experimental sites (Gudjr, Cadrn, and Alrts) and additional locations for uncertainty analysis (Touls and Drajn) (yellow circles) with associated climatic variability during the sunn hemp growing season (May–October) during 1999–2018. Gudjr: Guadajira, Spain (*Step C* and *D* of the workflow presented in Fig. 1); Touls: Toulouse, France (*Step D*); Cadrn: Cadriano, Italy (All Steps); Alrts: Aliartos, Greece (*Step C* and *D*), Drajn: Drajna Nouă, Romania (*Step D*). (For interpretation of the references to colour in this figure legend, the reader is referred to the Web version of this article.)

2017, with a volume of 200 mm at 7-day intervals until two months after sowing, due to the drought conditions (+2 °C of air temperature and −129 mm of precipitation compared to the mean values of the period 1999–2018). The abundant precipitation (mean of all the experiments, 345 ± 71.7 mm; Appendix B, Fig. B1-B4 in supplementary material) and high soil water retention capacity prevented supplemental irrigation during the 2016 and 2018 growing seasons.

The field trials carried out in Guadajira, a region of Extremadura, Spain (38° 51′ lat. N, 6° 40′ W, 222 m a.s.l) followed the same experimental design used in Cadriano 2017–2018. The soil in Guadajira was slightly acidic (pH 6.2) and loamy, with N, P, and K content of 0.7 g kg^{-1}, 14 mg kg^{-1}, and 54.7 mg kg^{-1}, respectively, and an organic matter content of about 0.8% (Appendix A, Table A2 in supplementary material). The seedbed was arranged using a disc plough, a cultivator tiller, and a rotary harrow by incorporating 32 kg ha^{-1} of N, 60 kg ha^{-1} of P_2O_5, and 60 kg ha^{-1} of K_2O. Two consecutive treatments of glyphosate (2 L ha^{-1}) and Stomp (pendimenthalin, 3 L ha^{-1}) were applied with a boom sprayer pre-sowing. Sunn hemp was drill-seeded at a density of 52 seeds m^{-2}. Experiment 14 (ID 14 in Table 1) was affected by pests (*Agriotes* spp. and *Spodoptera* spp.) at the very beginning of the growing season, thus requiring an additional application of Chlorpyrifos-Methyl 22.4% (m/v). No damage was observed on ID 15. Sunn hemp was drip-irrigated every three days, with an average irrigation water amount of 384 mm.

Five samplings were performed in Aliartos in a randomized complete block design (n = 4) in the period 2016–2018. The soil was moderately alkaline (pH 7.9–8.4) and sandy loam (Appendix A, Table A3 in supplementary material). The seedbed was prepared using a disc plough and a rotary harrow, incorporating 33 kg ha^{-1} of N, 45 kg ha^{-1} of P_2O_5, and 45 kg ha^{-1} of K_2O fertilizer. Weed control was performed pre-sowing using glyphosate at a concentration of 4 L ha^{-1} and post-emergence by hand hoeing. Sowing was carried out manually at 50 cm row spacing and three densities on the row: 5, 10, and 15 cm. A total of 323 mm of irrigation water was applied via drip irrigation during each growing season. Irrigation in Spanish and Greek experimental sites aimed at avoiding crop water stress, given the low precipitation during the May–October period (average cumulative precipitation of 141 mm in Guadajira and 186 mm in Aliartos in 2016–2018, compared to 345 mm in Cadriano; Appendix B, Fig. B4).

Daily air temperature (°C), precipitation (mm), radiation (MJ m^{-2} d^{-1}), and wind speed (m s^{-1}) of the three experimental sites were downloaded by the Prediction of Worldwide Energy Resources (POWER) at the NASA Langley Research Centre (Stackhouse, 2006), at a spatial resolution of 0.5° latitude by 0.5° longitude.

2.1.2. Methodology of field sampling

The field samplings provided the reference data used for model calibration and validation (Table 1). The sowing dates were classified as early (May) and late (June, after wheat harvesting). Likewise, harvest time was classified as early (i.e., August), medium (September), and late (October).

Phenological observations were collected at 50% emergence and 50% flowering stages. Plant density (plants m^{-2}) and AGB (Mg ha^{-1}) were measured twice at post-emergence and at harvest, respectively. AGB was assessed by sampling plants in a random 6 m^2 region of the plot, with subsequent oven-drying of the fresh mass at 105 °C until constant weight. Additional biometric parameters were monitored monthly in the 2017 and 2018 Italian experiments in a random plot area of 1 m^2, including leaf number (LN, number m^{-2}), branch number (BN, number m^{-2}), LAI, leaf width (LW, cm), and leaf length (LL, cm). The number of branches and leaves of each plant in the sample were separately counted for primary and secondary stems. In ID 9 and 10, LW and LL were measured at each sampling date on 20 expanding and 20 fully expanded leaves. LAI was determined by a destructive method using a LI 3100C area meter (LI-COR, Lincoln USA).

2.2. SunnGro: a process-based simulation model of sunn hemp

The Arungro model, specifically designed for giant reed (*A. donax* L.), was adapted to simulate sunn hemp to provide a new simulation model, SunnGro. Arungro simulates gross photosynthesis and respiration costs to estimate net carbon fixation, depending on radiation interception and crop transpiration. The original model provides a detailed description of LAI dynamics at shoot and plant levels, considering leaf width/length heterogeneity on a single tiller and among tiller cohorts. The evolution of tiller number is simulated based on thermal time, with the emission of new stems regulated by rhizome biomass during sprouting. While the algorithmic description of Arungro is provided in the original paper [33], a graphic representation of the processes implemented in SunnGro is shown in Fig. 3, which highlights the modifications with respect to the original model.

The SunnGro model was implemented in the BioMA framework (http://www.biomamodelling.org/) [37], which consists of platform-independent and reusable components, allowing for a modular representation of the agricultural systems. The main modifications in SunnGro were focused on the following: i) the estimation of flowering date via a linear, upper-limited response to daily temperature after emergence, optionally corrected for photoperiod [38], wherein the parameters driving phenological development represent the thermal time needed to reach flowering, cardinal temperatures for development (i.e. base and cutoff temperature), and day length for insensitivity and to inhibit flowering; ii) the simulation of the evolution of primary and secondary branches of sunn hemp, instead of considering the tiller population as in Arungro (Equation (1)); iii) the formalization of a specific function to estimate the number of leaves per plant (Equation (2)); iv) consideration of the elliptical shape of sunn hemp leaves, which were triangular in Arungro, in order to compute the leaf area; v) the impact of leaf senescence on LAI dynamics and on the daily rate of gross photosynthesis was switched off (in temperate environments sunn hemp is not able to reach the maturity stage by the end of the summer season, preventing leaf fall and seed formation [20]).

According to Bem et al. [32], BN (branch $plant^{-1}$; Equation (1)) and LN (leaf $plant^{-1}$; Equation (2)) were dynamically simulated using a three-parameter logistic function based on the thermal time ($\sum_{em}^{pbp} TT_i$, °C day) accumulated from emergence (em) to the peak of branch population (pbp), according to the following equations:

$$BN = 1 + \frac{SBN_{max}}{1 + e^{\left(-b_{SB} - k_{SB}\sum_{em}^{pbp} TT_i\right)}} \quad [1]$$

where, SBN_{max} (number $plant^{-1}$) is the maximum number of secondary branches per plant; b_{SB} and k_{SB} (unitless) are empirical coefficients modulating the steepness of BN accumulation and related to the rate of maturity/precociousness of the cultivar, respectively.

$$LN = 1 + \frac{LN_{avg}}{1 + e^{\left(-b_L - k_L\sum_{em}^{pbp} TT_i\right)}} \quad [2]$$

where, LN_{avg} (number $plant^{-1}$) is the average number of leaves per branch; b_L and k_L (unitless) are empirical coefficients modulating the steepness of LN accumulation and related to the rate of maturity/precociousness of the cultivar, respectively.

All the functions specific to the giant reed and sugar cane of Arungro were removed from SunnGro (i.e., lodging effect on light interception, stress days affecting green leaves, and anaerobic stress on root development). The algorithms accounting for the impact of water stress on root and branch development and on plant assimilation and growth were switched off until experimental datasets collected under contrasting rainfall and irrigation regimes were available. The SunnGro model is released as a Software Development Kit, including hypertext files documenting the implemented algorithms and software design and use. It

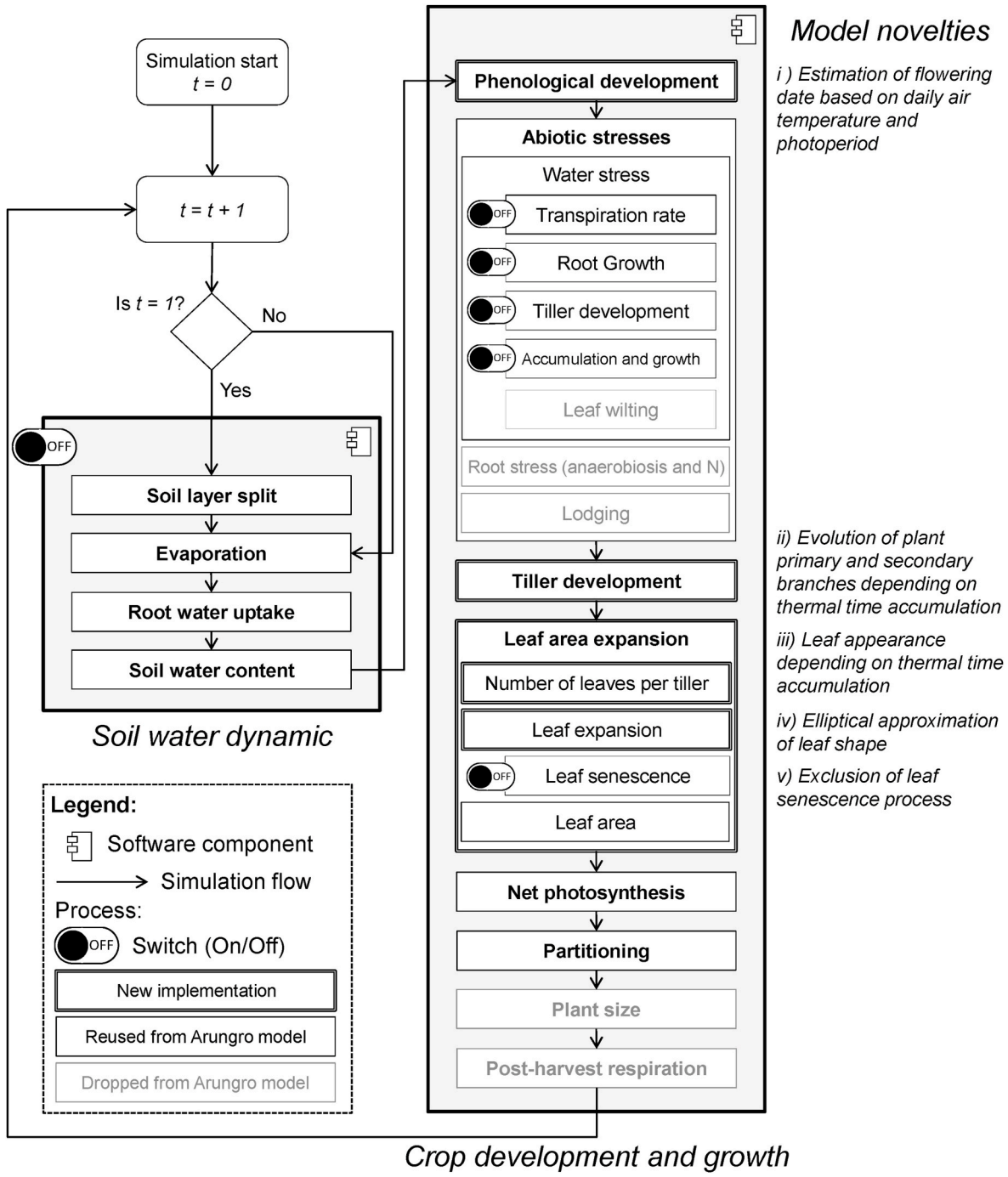

Fig. 3. Schematic representation of the main processes simulated by SunnGro. The simulation flow traces the execution order of sub-processes in a daily time step. The main processes are highlighted in bold, while sub-processes are reported in regular font. Double line boxes highlight changes to the original model. Boxes with a light grey border indicate processes that have been excluded from the seminal implementation.

also includes the code of a sample application showing how to use the software and run simulations in customized simulation experiments (Software availability section).

2.3. Simulation experiment design

According to the objectives of the BECOOL project, all simulations performed in model calibration and validation, as well as in the uncertainty analysis, were carried out under non-limiting conditions for water, nutrients, pests, and weeds, thus considering only temperature and radiation as limiting factors (i.e., potential level) [39]. To achieve the maximum crop yield potential in the area, sunn hemp was constantly irrigated in Greek, Spanish, and some Italian experiments, thus preventing the possible incidence of water stress during critical phenological phases. The assumption that nutrient availability is unlimited is consistent with the N-fixing ability of the crop and with findings from Parenti et al. [36], who proved the absence of significant yield differences between fertilized and unfertilized sunn hemp in Cadriano.

2.3.1. Model calibration and validation

SunnGro was calibrated using the data collected in Cadriano in experiments conducted from 2016 to 2018 (IDs 1–4 and 9–13 in Table 1).

The phenological development was set by manually tuning the thermal time needed to reach flowering according to field observations. Subsequently, the parameters connected to BN, LN, leaf expansion, and photosynthesis were varied within the biophysical ranges reported in the literature and available from experimental data to increase model accuracy (Table 2). The multi-start downhill simplex [40] was used as the optimization algorithm to generate a simplex, a geometrical figure with N+1 vertices, with N as the parameter number under calibration. The average root mean square error [RMSE; minimum (min) and optimum (opt) = 0, maximum (max) = +∞] [41] was chosen as the objective function and evaluated after each simulation run. The automatic optimization ended when the difference in RMSE between consecutive simulations fell below a tolerance range; 20 simplexes, 100 iterations, and a tolerance of 0.01% were set as operational settings.

A multi-site validation was carried out to test the accuracy of SunnGro across experimental sites. The parameter set derived from model calibration was used and SunnGro performances were tested using the AGB measurements from field trials carried out in Cadriano (IDs 5–8), Guadajira (IDs 14–15), and Aliartos (IDs 16–20) in the period 2017–2018 as reference variables.

The model performances in calibration and validation were quantified with standard metrics used in crop modeling studies: the RMSE, relative root mean square error (RRMSE, min and opt = 0%; max = +∞) [42], coefficient of residual mass (CRM, min = −∞, max = +∞, opt = 0, unitless) [43], modeling efficiency (EF, min = −∞, opt and max = 1, unitless) [44], and coefficient of determination (R^2, min = 0, opt and max = 1, unitless) [45].

2.3.2. Exploring SunnGro behavior under different agro-environmental conditions

An uncertainty analysis of SunnGro outputs was carried out at five European sites by performing simulations during 1999–2018. The aim was to explore model responses under varying climatic and management conditions, in order to investigate model behavior and derive agronomic indications on crop suitability and on the most promising management strategies in European environments. In this context, the introduction of a new high-yield, low-input, and multi-purpose species represents an interesting option to increase crop diversification and the multifunctionality of the agricultural sector.

With respect to the scope, three out of five simulation sites were the same as those used in calibration/validation (i.e., Cadriano, Guadajira, and Aliartos), while two additional locations were selected in South Western (Toulouse, France; 43°36′ lat. N, 1° 26′ E, 141 m a.s.l.) and South Eastern (Drajna Nouă, Romania; 44°25′ lat. N, 27° 25′ E, 37 m a.s.l.) Europe (Fig. 2). The choice of sites was driven by study of the available information on i) European climate classification according to the Köppen-Giger taxonomy (KGT) [46], ii) presence of reliable, consistent and accessible data sources for weather and crop management, and iii) potential suitability of the crop to agro-climatic conditions. The analysis of the most represented KGT climate in South Western and Eastern Europe led to the identification of three different climate zones, corresponding to a hot-summer Mediterranean climate (*Csa*, Aliartos and Guadajira), marine west coast climate (*Cfb*, Toulouse), and humid subtropical climate (*Cfa*, Drajna Nouă and Cadriano). While *Cfa* and *Cfb* climates are characterized by very favorable precipitation amounts during the sunn hemp growing season (average always higher than 310 mm), as well as suboptimal growth temperature (19.4 °C < mean temperature < 21.6 °C, mean standard deviation, SD, of 4.7 °C), *Csa* is drier (average precipitation of 160 mm, SD = 51.7 mm) but characterized by thermal regimes that are closer to the optimum for the species (22.7 °C < mean temperature < 23.6 °C, SD = 5 °C) [30]. The site-specific daily mean air temperature (°C), radiation (MJ m^{-2}), and precipitation (mm) data in the period were retrieved from the NASA POWER database at a 0.5-degree resolution, as in the case of calibration and validation activities. Data are validated, bias-corrected, and harmonized automatically according to the international guidelines for hydro-meteorological data, and thus, are not affected by inconsistencies related to the adoption of i) different measurement instruments and calibration methods and ii) alternative data reconstruction procedures in the presence of outliers, missing data, and/or even when key target variables are not measured. In addition to the well-known reliability as input data for agricultural studies at both regional and national spatial scales [47], NASA POWER data proved to be representative of local temperature and radiation trends in the study areas, although they do not explicitly account for sub-grid scale issues related to clouds or topography. A comparison between the meteorological station and NASA POWER data for the three experimental sites is shown in Appendix C, Fig. C1 in the supplementary material. In brief, as the data measured by Italian and Spanish stations presented several missing/aberrant temperature/radiation data, we decided to use NASA POWER products. Greek station data were rejected because radiation measurements were not available and the distance between the experimental plot and the closest meteorological station was more than 14 km, which is regarded as the "maximum threshold beyond which it was no longer possible to consider the weather described by the station as being sufficiently representative of that of the field" [48]. An overview of weather variable patterns in all sites in the period 1999–2018 is given in Fig. 2.

For each experimental site, the simulated i) AGB at harvest, ii) time to reach the peak of BN (TPBN, days), and iii) the total number of days in which new leaves are emitted (TPLN, days) were selected as target variables, while average air temperature and sowing time were selected as explanatory weather and management factors, respectively. For temperature, the range of variation was defined using the 20 mean yearly values in the period 1999–2018 (May–October), corresponding to a thermal interval between 19 and 27 °C. A climatic series of 20 years was considered representative of the current daily, seasonal, and interannual weather fluctuations, as well as most of the less frequent climate events that may occur in a given agro-ecosystem [49,50]. Nine planting strategies were tested, by anticipating/delaying the standard sowing time (June 15, day of the year 166, DOY) by 1–4 weeks (i.e., from May 18, DOY 138 to July 13, DOY 194).

Although very few studies are available in the literature on the cultivation of sunn hemp in Mediterranean countries, all locations are suited for growing soybean, which is part of the same botanical family and has similar physiological and agronomic requirements (cultivation period, plant density, and fertilization) to those of sunn hemp [12,51].

The model outputs were analyzed using boxplots; ggplot2 R package, version 0.9.3 [52] and contour plots (NCSS Statistical software; https://www.ncss.com/).

Boxes expand from the 25th to 75th percentile (interquartile distance, IQD), with the centerline fixed at the 50th percentile; whiskers expand to the most extreme data points, the distance to which is 1.5 times lower or higher than the length of the box. Outliers are represented as points. Contour plots are graphical representations of the relationships among three numeric variables in two dimensions.

3. Results

3.1. Model performances in reproducing sunn hemp development and growth

The simulated dynamics of BN and LN and AGB and LAI for the field trials used for calibration are presented in Figs. 4 and 5, respectively. SunnGro correctly reproduced the observed dynamics under alternative combinations of SD and harvest time (HT), with an RMSE on the flowering date equal to 3.6 days (number of trials, n = 5). The model accurately simulated the evolution of biometric traits (i.e., BN and LN) along the vegetative season (Fig. 4) in all experiments, with slight errors for the LN (RMSE = 2.09 branches $plant^{-1}$ for BN and 35.83 leaves $plant^{-1}$ for LN; RRMSE = 37.04% for BN and 27.24% for LN). Indeed, SunnGro explained 80% and 92% of the year-to-year variability of BN

Table 2
SunnGro parameter list. Parameter values marked with an asterisk were set to defaults reported in the literature, while the remaining ones were calibrated within ranges defined by the literature or obtained from experimental results (E).

Parameter name	Description	Min	Max	Value	Unit	Reference
Phenology						
TBaseEmerg	Base temperature for emergence from planting	8 (3)	9.2 (16)	9.47	°C	[53], ([54])
TCutOffEmerg	Optimum temperature for emergence from planting	28	43	30	°C	[54]
TTEmergFlower	Thermal time from emergence to flowering	47.34	63.94	63	°Cd	E[a,b]
TBaseFlower	Base temperature for flowering	8	11	9.41	°C	[55]
TCutOffFlower	Optimum temperature for flowering	27	29	28	°C	[55]
DayLenghtIf	Day length threshold above which no accumulation of physiological time occurs			14*	hour	[38]
DayLenghtIns	Day length threshold below which maximum physiological time accumulation occurs			6*	hour	[38]
TTPlantEmerg	Thermal time from planting to emergence	47	64.29	59.15	°Cd	E[a,c]
Branch emission						
TBaseBranchDevelop	Base temperature for branch population development	5.95	8.05	6.72	°C	[56] [d]
TCutOffBranchDevelop	Optimum temperature for branch population development	30	45 (even >)	38.35	°C	[56]
TTEmergPeakBranchPop	Thermal time from emergence to peak branch population	1037	1500	1318.48	°Cd	E[a]
SBNmax	Maximum number of secondary branches per plant	2	36	25.87	unitless	E
kSB	Empirical parameter of the logistic function for branch emission	–	–	0.007683	unitless	E[e]
bSB	Empirical parameter of the logistic function for branch emission	–	–	−9.4960	unitless	E[f]
Leaf appearance						
TBaseLeafEmission	Base temperature for leaf emission	8.9	10.9	9.48	°C	[53]
TCutOffLeafEmission	Optimum temperature for leaf emission	30	35	30.45	°C	[57]
LNavg	Average number of leaves per branch	2	87.5	25.87	unitless	E
kL	Empirical parameter of the logistic function for leaf appearance	–	–	0.0651	unitless	E[g]
bL	Empirical parameter of the logistic function for leaf appearance	–	–	−7.6870	unitless	E[h]
Leaf area extension						
MaxNumGreenLeavesWW	Maximum number of green leaves per branch under well water conditions			30*	unitless	cd
MeanLeafLength	Mean leaf length	3.06	11.9	11.65	cm	E[i]
MeanLeafWidth	Mean leaf width	6	32.4	29.86	mm	E[j]
Photosynthesis						
TBasePhotosynthesis	Base temperature for photosynthesis	0	10	5.88	°C	[56]
FractGrossPhotoGroResp	Fraction of gross photosynthesis lost for growth respiration	0.19	0.31	0.238	unitless	[56]
TBaseRootExtension	Base temperature for root extension	0	10	6.22	°C	[56]
TCutOffRootExtension	Optimum temperature for root extension	24	33	30.45	°C	[58]
RefMaintResp	Maintenance respiration at 10 °C	0.01	0.03	0.011	Mg Mg^{-1} d^{-1}	[56]
MaxPartFractAerialDM	Maximum partition fraction to aerial dry mass	0.5	1	0.987	Mg Mg^{-1}	E
MaxRadConvEfficiency	Maximum radiation conversion efficiency	0.95	8.68	6.55	g MJ^{-1} d^{-1}	[59,60] [k]
PARExtCoeff	PAR extinction coefficient	0.826	0.91	0.83	unitless	[61]
PartCoeff	Coefficient of the exponential function for aerial dry mass partitioning	0.51	0.69	0.497	unitless	[33] [l]
MinPartFractAerialDM	Minimum partition fraction to aerial dry mass	0	0.19	0.0483	Mg Mg^{-1}	E
RootLengthMassRoot	Root length per unit root mass	7650	10350	9014	cm g^{-1}	[38] [m]
MaxRootLengthDensity	Maximum root length density	1	2.8	1.858	cm cm^{-3}	[62] [n]
MinRootLengthDensity	Minimum root length density	0.4	0.8	0.724	cm cm^{-3}	[62] [o]
RootDepthIncreaseGDD	Root depth increase per growing degree day	0	1.2	0.57	cm °Cd	[57] [p]
CropCoeff	Crop water use coefficient			1.05*	unitless	[63]
Q10ForMaintResp	Fractional increase in respiration rate per 10 °C rise in temperature			2*	unitless	[57]

Literature pertaining to *Crotalaria juncea* L.: [53]; *Vigna unguiculata* (L.) Walp.: [54–56,58,61–63]; *Glycine max* (L.) Merrill: [56,57]; *Pisum sativum* L.: [59]; generic defaults: [33,38,60]; cd) custom defined.

Notes.

[a] Tbase = 10 °C, Tcutoff = 25 °C.

[b] Range: ±15% around experimental default (55.69).

[c] Range: ±15% around experimental default (55.9).

[d] Range: ±15% around default value (7).

[e] Autotune calibration (AC) performed starting from experimental default (0.0084).

[f] AC performed starting from experimental default (−7.1463).

[g] AC performed starting from experimental default (0.0111).

[h] AC performed starting from experimental default (−10.3421).

[i] Boundaries estimated as experimental mean value (7.48) ± 1.5SD.

[j] Boundaries estimated as experimental mean value (19.2) ± 1.5SD.

[k] Boundaries of gross photosynthesis (GP) rate were estimated by multiplying net photosynthesis (NP) rate' boundaries (min: 0.57, max: 4.34, as reported in i) by GP/NP ratio (derived from l, min: 1.67, max: 2).

[l] Range: ±15% around default value (0.6).

[m] Range: ±15% around default value (9000).

[n] Upper layer.

[o] Lower layer.

[p] Upper limit.

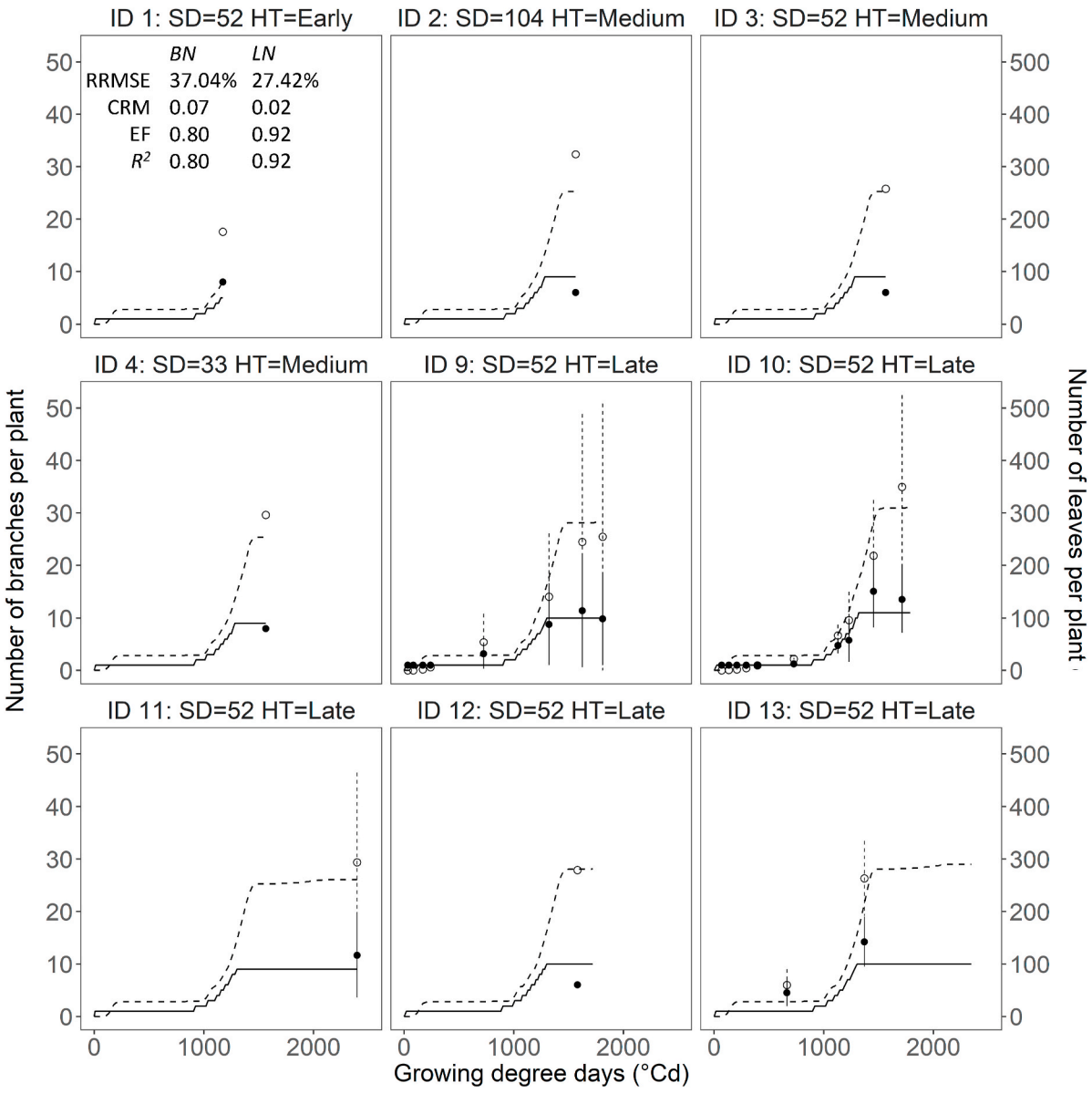

Fig. 4. Model performances in reproducing the dynamics of the number of branches (BN, continuous line, main axis) and of leaves (LN, dashed line, secondary axis) per plant during the vegetative season of sunn hemp (May–October). Measured BN (black dots) and LN (empty dots) were collected in the period 2016–2018 at Cadriano (Northern Italy) from plots with different combinations of sowing density (SD, plants m^{-2}) and harvest time (HT). The vertical bars correspond to the standard deviation of sampled mean (n = 4). The evaluation metrics reported in the top left corner are the relative root mean square error (RRMSE, %), modeling efficiency (EF, unitless), coefficient of residual mass (CRM, unitless), and coefficient of determination (R^2, unitless). IDs are listed in Table 1.

and LN (EF = 0.80 for BN and 0.92 for LN). Larger errors corresponded to the early harvested experiment in 2016, where SunnGro underestimated LN (i.e., −95 leaves $plant^{-1}$), despite BN being correctly simulated (i.e., −3 branches $plant^{-1}$). CRM values indicated no systematic bias for BN and LN (CRM = 0.067 for BN and 0.021 for LN). Nevertheless, the simulation results indicated a frequent underestimation of BN at the early vegetative stages (around 750 GDD from emergence), which resulted in an underestimation of LN at the same phenological stage.

The proper simulation of BN and LN led to good results for LAI and AGB dynamics during the growing season (Fig. 5; RMSE = 1.35 m^2 m^{-2} for LAI and 1.81 Mg ha^{-1} for AGB; RRMSE = 33.10% for LAI and 21.36% for AGB). Thus, SunnGro was capable of describing the trends observed for the AGB data in six out of nine experiments (EF = 0.78), with the exception of ID 2, 4 (medium harvest), and 10 (late harvest), where it overestimated the reference data. The LAI simulation was slightly less accurate than that of the AGB, with EF = 0.62. Compared to LN, the model explanatory power was lower, decreasing to 82% for AGB and 71% for LAI. The underestimation of LN in the early vegetative phase delayed the LAI increase (e.g., ID 9 and 13 in Fig. 5) before the maximum number of branches was reached.

SunnGro accurately reproduced the decrease in LAI and AGB according to the lower SD, from high (i.e., 104 plants m^{-2}) to medium and low (i.e., 52 and 33 plants m^{-2}) SD (e.g., ID 2, 3, and 4 in Fig. 5), and was also able to model the higher AGB in late harvesting at medium SD (e.g., ID 1, 9, and 13 in Fig. 5).

In summary, *Step A* activities (Fig. 1) led to a detailed and accurate representation of plant development and growth, while markedly reducing the number of parameters from 84 (Arungro) to 38 (SunnGro; Table 2).

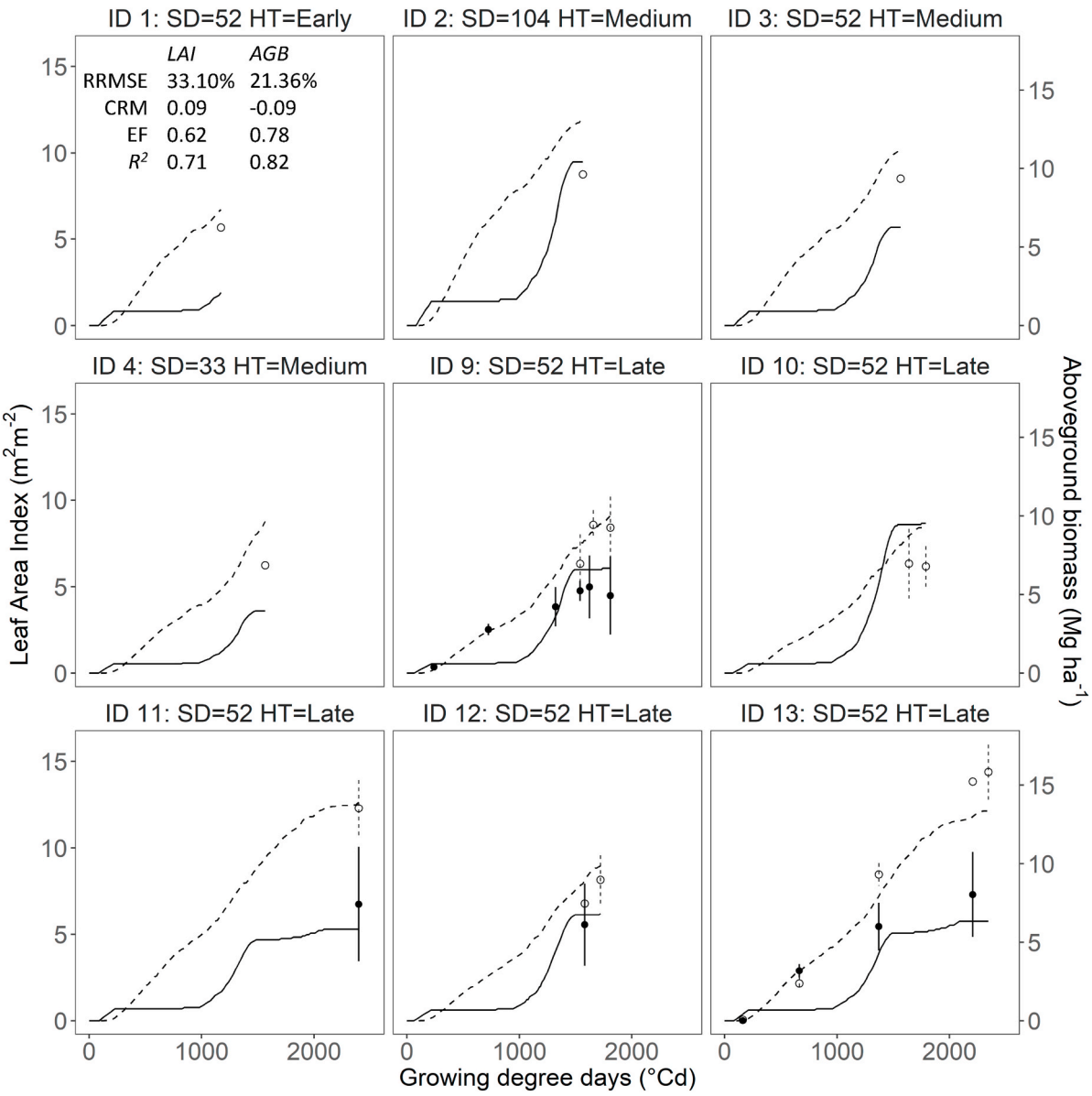

Fig. 5. Model performances in reproducing the dynamics of the leaf area index (LAI, continuous line, main axis) and aboveground biomass (AGB, dashed line, secondary axis) during the vegetative season of sunn hemp (May–October). Measured LAI (black dots) and AGB (empty dots) were collected in the period 2016–2018 at Cadriano (Northern Italy) from plots with different combinations of sowing density (SD, plants m^{-2}) and harvest time (HT). Vertical bars correspond to the standard deviation of sampled mean (n = 4). The evaluation metrics reported in the top left corner are the relative root mean square error (RRMSE, %), modeling efficiency (EF, unitless), coefficient of residual mass (CRM, unitless), and coefficient of determination (R^2, unitless). IDs are listed in Table 1.

3.2. Multi-site model validation

The comparison of measured and simulated AGB (Mg ha^{-1}) in the Aliartos, Guadajira, and Cadriano experiments in the period 2016–2018 is shown as a scatterplot in Fig. 6. The model validation was carried out by applying the model parameter set calibrated in *Step B* of this study (Fig. 1; Table 2).

SunnGro performances in simulating AGB were positive ($R^2 = 0.67$), confirming its ability to reproduce the large inter-annual variability of the field experimental data in the explored conditions (RMSE = 3.02 Mg ha^{-1}, RRMSE = 20.39%, EF = 0.6, and CRM = 0.08). The model slightly underestimated the higher AGB in the Aliartos experiments (14.00 Mg ha^{-1}<AGB<21.67 Mg ha^{-1}), while correctly reproducing the increasing trend from low (31.5 plant m^{-2}) to medium (46.3 plant m^{-2}) and high (89 plant m^{-2}) SD, as well as the lowest AGB in the late sowing experiment (ID 20, Fig. 6). In Guadajira, SunnGro simulated lower AGB (7.06 Mg ha^{-1}<AGB<9.6 Mg ha^{-1}), despite a systematic overestimation of the experimental data (about 3.4 Mg ha^{-1}). The model also succeeded in simulating the Cadriano experiments (8.91 Mg ha^{-1}<AGB<18.79 Mg ha^{-1}), except in late sowing and the late harvest time trial in 2016 (ID 8 Fig. 6, underestimation of 5.2 Mg ha^{-1}), and in the early sown, medium harvested trial in 2018 (ID 7; Fig. 6, overestimation of 3.34 Mg ha^{-1}). The average differences between the simulated and reference data fluctuated around −2.4 Mg ha^{-1} for Cadriano (−5.23 Mg ha^{-1}< AGB<3.34 Mg ha^{-1}), 3.45 for Guadajira (2.78 Mg ha^{-1}<AGB< 4.12 Mg ha^{-1}), and −1.93 for Aliartos (−2.23 Mg ha^{-1}<AGB < −1.65 Mg ha^{-1}) and were always smaller than the standard deviation of sampled mean (Fig. 6).

3.3. Uncertainty analysis

While both the boxplots and contour plots of AGB are presented in

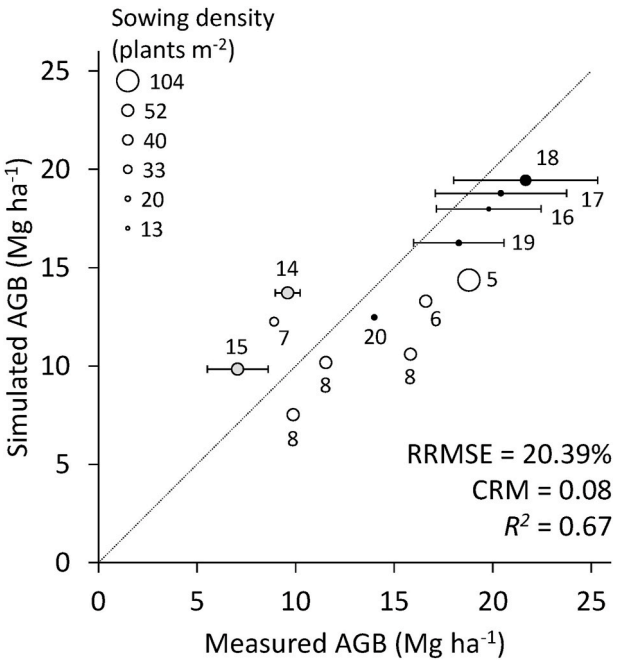

Fig. 6. A 1:1 plot between measured and simulated values of aboveground biomass (AGB) of sunn hemp in Aliartos (black circles), Cadriano (empty circles), and Guadajira (grey circles) in the period 2016–2018. Samples are labelled with trial ID. Circle size is proportional to sowing density (plant m^{-2}). Horizontal bars correspond to the standard deviation of sampled mean (n = 4). The evaluation metrics reported in the bottom right corner represent the relative root mean square error (RRMSE, %), coefficient of residual mass (CRM, unitless) and coefficient of determination (R^2, unitless). The dotted line represents the 1:1 fit (perfect fit).

this section, those referring to i) the time to reach the peak of BN and ii) the total number of days in which new leaves are emitted are reported in the supplementary material (Appendix D, Fig. D1, D2, D4, and D5).

Fig. 7 presents the simulated AGB in the long-term simulation experiments carried out in Guadajira, Aliartos, Cadriano, Drajna Nouă, and Toulouse in the period 1999–2018 to analyze model uncertainty. The results revealed two distinct groups of sunn hemp productivity, the former corresponding to the simulations performed in Aliartos and Guadajira, with the 20-year average AGB in the range 12.1–14 Mg ha^{-1} (average = 13.27 Mg ha^{-1}), with a small variability (0.44 < average IQD< 0.84 Mg ha^{-1}; mean = 0.64 Mg ha^{-1}). The second group included simulations performed in Cadriano, Drajna Nouă, and Toulouse, leading to AGB values ranging from 8.4 to 11.9 Mg ha^{-1} (average = 10.41 Mg ha^{-1}), with a larger variability (on average 0.73 < IQD<1.38 Mg ha^{-1}; mean = 0.97 Mg ha^{-1}). Guadajira was the site where simulated AGB was the highest and more stable, whereas the simulated AGB in Cadriano (average IQD of 1.23 Mg ha^{-1}, 67% higher than the mean of the other sites) and Toulouse (average AGB of 9.87 Mg ha^{-1}, 17% lower than the mean of the other locations) were the lowest and the most variable.

The simulated average AGB increased with SD level, from low (10.33 Mg ha^{-1}), to medium (11.57 Mg ha^{-1}) and high (12.71 Mg ha^{-1}). Conversely, AGB variability decreased from high (IQD = 0.95 Mg ha^{-1}) to medium (0.82 Mg ha^{-1}) and low SD (0.74 Mg ha^{-1}). The only exception was in Toulouse, where AGB variability did not vary among SD levels, with IQD ranging from 0.77 to 0.81 Mg ha^{-1}. Simulated AGB decreased linearly as the sowing date was delayed, ranging from 14.13 Mg ha^{-1} at DOY 138 (May 18) to 9.22 Mg ha^{-1} at DOY 194 (July 13), while the average IQD increased from 0.78 to 0.97 Mg ha^{-1}. The most marked IQD linear increases were achieved in Guadajira and Cadriano (linear slope of about 0.062 Mg ha^{-1}; 0.57 < R^2 < 0.62), and to a lesser extent, in Aliartos and Drajna Nouă (linear slope of about 0.025 Mg ha^{-1}; 0.27 < R^2 < 0.68), while in Toulouse it remained practically unchanged (linear slope of 0.009 Mg ha^{-1} and R^2 very close to 0).

The combined effect of temperature and sowing date on the variability of sunn hemp productivity was further investigated using contour plots (Fig. 8).

In general, the simulated AGB progressively increased from late to early sowing, and from lower to higher average air temperatures, following the order Toulouse < Drajna Nouă < Cadriano < Aliartos < Guadajira for the sites and low < medium < high for SD.

In Guadajira and Aliartos, the postponing of the sowing date had a larger effect than temperature, leading to lower AGB variability

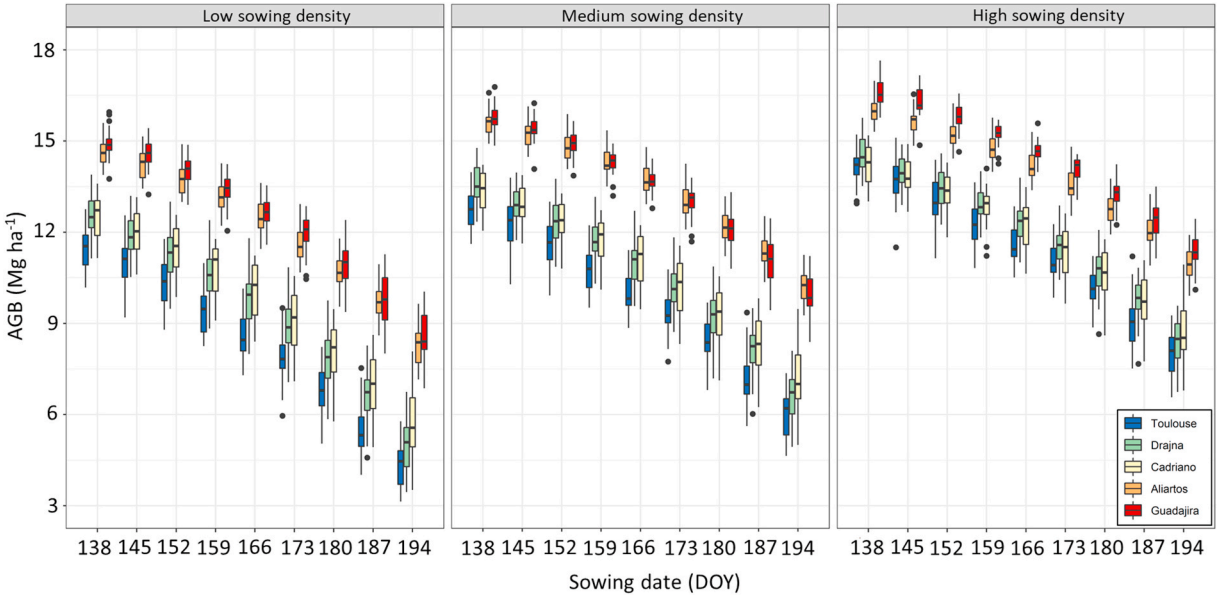

Fig. 7. Distribution of aboveground biomass (AGB, Mg ha^{-1}) simulated at harvest in Guadajira (Spain; red box), Aliartos (Greece; orange box), Cadriano (Italy; yellow box), Drajna Nouă (Romania; green box), and Toulouse (France; blue box) in the period 1999–2018, by adopting different sowing dates (nine periods between DOY 138 and 194) and densities (low = 33 plants m^{-2}, medium = 52 plants m^{-2}, and high = 104 plants m^{-2}). Color gradient (i.e., from red to blue) mirrors the increasing trend of cumulative radiation during sunn hemp season (May–October). Each box is derived from the values simulated at harvest for each of the 20 years. (For interpretation of the references to colour in this figure legend, the reader is referred to the Web version of this article.)

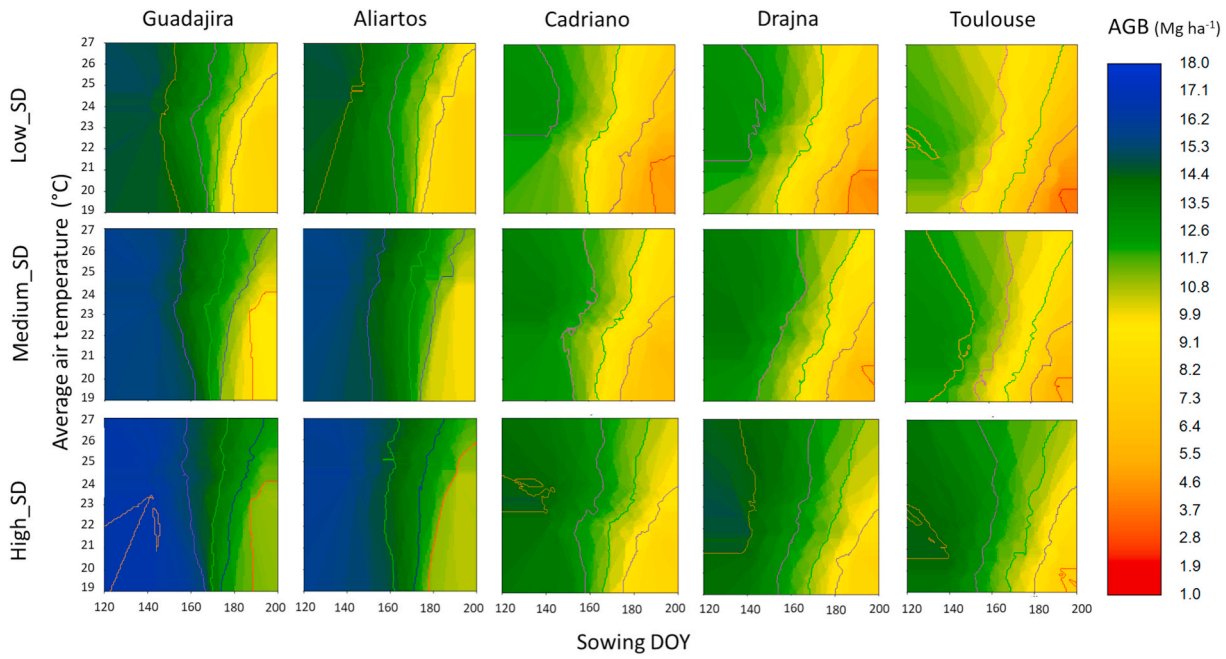

Fig. 8. Simulated aboveground biomass (AGB, Mg ha^{-1}) as a function of mean air temperature during the crop cycle (y-axis, °C) and sowing time (x-axis; nine dates between DOY 138 and 194) at the Spanish (Guadajira), Greek (Aliartos), Italian (Cadriano), Romanian (Drajna Nouă), and French (Toulouse) sites in the period 1999–2018. SD: Sowing density (low = 33 plants m^{-2}, medium = 52 plants m^{-2}, and high = 104 plants m^{-2}).

compared to Cadriano, Drajna Nouă, and Toulouse.

In Guadajira and Aliartos, early sowings (before DOY 160 at high SD, 150 at medium SD, and 140 at low SD) led to the highest AGB, regardless of temperature conditions, during the growing season and reduced the AGB uncertainty (expressed as IQD) from 8.33 to 2.5 Mg ha^{-1} at Guadajira and from 7.6 to 2.5 Mg ha^{-1} at Aliartos. In both sites, late sowings (i.e., after DOY 180) allowed the collection of similar AGB values than in Cadriano, Drajna Nouă, and Toulouse using standard planting dates (DOY 166) and medium/high SD. Cadriano, Drajna, and Toulouse presented similar and larger AGB variability compared to Guadajira and Aliartos because of the higher temperature effect on sunn hemp productivity. The uncertainty due to temperature on AGB variability increased in delayed sowing, ranging from 2.27 Mg ha^{-1} (DOY 138) to 4.39 Mg ha^{-1} (DOY 194) at Cadriano, from 2.48 Mg ha^{-1} (DOY 138) to 3.1 Mg ha^{-1} (DOY 194) at Drajna Nouă, and from 2.4 Mg ha^{-1} (DOY 138) to 2.7 Mg ha^{-1} (DOY 194) at Toulouse, with slight differences among sowing densities. For a 1 °C temperature increase, the variability of simulated AGB at medium SD increased in a range from 0.70 (Toulouse) to 0.76 Mg ha^{-1} (Drajna Nouă) at DOY 138 and from 0.89 (Toulouse) to 1.4 Mg ha^{-1} (Cadriano) at DOY 194.

4. Discussion

4.1. Rationale and methodology of model parameterization

SunnGro parameters related to phenology and growth were adjusted within their biophysical ranges of variation during model calibration, using data from the literature and the experimental data collected in Cadriano (Table 2). When no data for sunn hemp were available, the parameter ranges were taken from other legume crops, such as cowpea, pea, and soybean. The base temperature for emergence (9.5 °C) was consistent with that identified by Qi et al. [53], while the optimum temperature was set to 30 °C according to the data available on cowpea [54]. The thermal sum from sowing to emergence was set to 59 GDD, and the range in variation of this parameter (47–64 GDD) was set according to field measurements (ID 9). A dedicated function to simulate the flowering date considering the photoperiod sensitivity of the short-day sunn hemp crop was included in SunnGro [38]. The base and cutoff temperatures for flowering were set at 9.4 and 28 °C, respectively, according to Craufurd et al. [55], whereas the minimum and maximum day lengths were set at 14 and 6 h, respectively [38]. The dynamics of branches were reproduced by a three-parameter logistic function [32], based on thermal time accumulation from emergence to the peak of the branch population, with base (6.72 °C) and optimum temperatures (38.35 °C) in line with Boons-Prins et al. [57] and Van Heemst [56] for soybean. The average number of leaves per plant was set at 26, varying the base and optimum temperatures coherently with Qi et al. [53] on sunn hemp and Boons-Prins et al. [57] on soybean. Average leaf length (11.7 cm) and width (3 cm) were set according to the field measurements (ID 9). The maximum conversion coefficient of the PAR intercepted into dry matter was calibrated to 6.55 g MJ^{-1} d^{-1} [59,60], reflecting the higher productive attitude of sunn hemp compared to other legume crops. The base temperature for photosynthesis (5.9 °C), fraction of gross photosynthesis lost for growth respiration (23.8%), maintenance respiration at 10 °C (0.011 Mg Mg^{-1} d^{-1}), and base temperature for root extension (6.22 °C) were consistent with the measurements of Van Heemst [56] on cowpea and soybean. In addition, the optimum temperature for root extension (30.45 °C), increase in root length per unit of root biomass (9014 cm g^{-1}), root depth increase per growing degree day (0.57 cm °C day), and maximum (1.858 cm cm^{-3}) and minimum (0.724 cm cm^{-3}) root length density were consistent with data reported by Dart and Mercer [58], Stöckle et al. [38], Boons-Prins et al. [56], and Moroke et al. [62], respectively. The maximum (0.987 Mg Mg^{-1}) and minimum (0.0483 Mg Mg^{-1}) partitioning coefficients of aerial dry mass were set according to reference experimental data and data from studies by Bem et al. [31,32] and Abdul-baki et al. [13]. The PAR extinction coefficient was derived by applying the LAI measurements and light intercepted data from the ID 9 experiment to the Lamber-Beer equation and were in line with the reference value for cowpea [61]. The fractional increases in respiration rate per 10 °C rise in temperature (Q10) was left to the default value according to Boons-Prins et al. [57] for *Pisum sativum* L. The only range taken from the Arungro model was related to the coefficient of the exponential function for aerial dry mass partitioning (between 0.51 and 0.69).

4.2. Model performance in reproducing field experiments

The accuracy of SunnGro in simulating biometric and growth variables was satisfactory and in line with modeling studies available in the literature. Bem et al. [31,32] estimated the leaf number per plant and total dry matter (TDM) content in the Brazilian Rio Grande do Sul State, with R^2 values ranging from 0.71 to 0.85 for LN and 0.53 to 0.69 for TDM. The poor accuracy in simulating late sowing datasets obtained by these models was probably due to the use of empirical relationships based on the number of days from sowing, without explicitly considering i) the variability of pedo-climatic conditions, ii) processes connected to growth and development, and iii) interactions between environmental and management practices. Furthermore, the empiricism characterizing available models reduces their range of applicability, which is limited to the conditions in which they were developed [64]. This is an essential prerequisite for model reuse on other species/varieties, regions/locations, spatial scales (smaller/larger than in calibration) [65], and climate change impact assessment studies [66].

Low accuracy ($R^2 = 0.37$) was obtained by Le et al. [30], who used the EPIC model to simulate the rainfed yield of sunn hemp grown as a single cover crop or intercropped with millet in diversified crop rotations in Cambodia. These results were affected by the following: the high complexity of the conservation system simulated, the oversimplified approach used to represent canopy structure/development, and lack of extensive datasets for model calibration (ten experiments). Indeed, EPIC is a generic simulator that does not consider either the simulation of leaf size heterogeneity or the representation of the dynamic daily evolution of branch/leaf populations depending on weather and management conditions, in turn affecting light interception, photosynthesis rate, and biomass accumulation. Furthermore, the calibration dataset did not include multiple in-season measurements of phenology and growth variables, as well as detailed information to define crop management and model parameterization.

All these considerations support the development of a specific process-based model accounting for the heterogeneity of sunn hemp canopy architecture and its evolution over time. Our methodology implied the formalization of new algorithms targeting crop-specific traits and a novel parameterization supported by an extensive literature search and field data collection. This is a standard procedure in crop modeling studies and has already been applied for oilseed crops [67–69] and legume species [25,26]. Our study produced very accurate results in simulating sunn hemp productivity across environments, while decreasing the complexity of the original model by halving the number of parameters. At the field scale, the generic legume models explained about 60–81% of inter-annual AGB and yield variability, with increasing uncertainty from potential to water- and nitrogen-limited conditions. Compared to generic simulators, specific legume models [27,29] performed even better, although tested with calibration datasets, including a limited number of varieties and in a few sites and years.

4.3. Scenario analysis

The potential of sunn hemp as feedstock for advanced biofuel or as a soil improver in Europe needs to be primarily investigated from an agronomic standpoint, especially from the perspective of climate change. Indeed, the ideal energy crop should i) provide the highest biomass yields when cultivated as a double crop, in order to ii) avoid competition with food/feed crops and iii) provide stable (or even increasing) yields in the long-term, possibly minimizing the inputs/cost needed to achieve these yields. The presented scenario analysis (Fig. 7) was intended to both explore model behavior and answer these research questions. This provides the basis for the use of SunnGro as a supporting tool for farmers and green energy sector stakeholders/researchers to optimize management practices and to assess AGB trends across geographical areas and climatic scenarios in light of biogas and bioethanol production. For these reasons, AGB was simulated in five environments representative of Southern and Eastern Europe using 20 years of weather data and different sowing densities and dates. In this light, sunn hemp productivity as a main or double crop can be estimated by using the May and July sowings as representatives for the two use cases, respectively. Indeed, since winter cereals in the study areas are generally harvested in June, sunn hemp sown as a double crop at the beginning of July could be a valid option to increase the productivity of existing cropping schemes [15]. In this regard, potential biomass productivity fluctuated around 17 Mg ha^{-1} as the main crop and 10 Mg ha^{-1} as a double-crop in Aliartos and Guadajira, and about 15 Mg ha^{-1} and 7 Mg ha^{-1} in Cadriano, Drajna Nouă, and Toulouse. Indeed, while in hot-summer Mediterranean Spanish and Greek environments, sunn hemp demonstrated a high yield potential, our simulations show that sub-optimal temperatures limit its productivity in the marine west coast (i.e., Toulouse) and humid subtropical climates (Cadriano and Drajna Nouă). In the latter countries, projected temperature increases are expected to favor the crop by reducing the thermal limitation and hastening leaf area expansion in the early crop stages, in turn enhancing light interception. Conversely, in Aliartos and Guadajira, climate change conditions would presumably increase the crop water requirements, given the 300–400 mm of irrigation water needed under the current climatic conditions. Finally, in a sustainable low-input sunn hemp cultivation scenario, stakeholders must comply with the following guidelines: i) select areas where precipitation can meet sunn hemp requirements (similar to the sites in Cadriano and Drajna Nouă); ii) perform quick seedbed preparations after the main crop and plant as soon as possible to enlarge the sunn hemp growth cycle; iii) choose high sowing densities, regardless of site and sowing time, to maximize yields and approach the potential yield of 15 Mg ha^{-1} reached in Cadriano.

4.4. Final remarks and areas of improvement

The collection of reference experimental data and growth variables carried out at multiple sites under optimal agronomic management for sunn hemp prevented the testing of the impact of abiotic and biotic stresses on biomass accumulation. Furthermore, the capability of SunnGro to simulate the impact of soil nitrogen availability on sunn hemp is constrained by the availability of i) a ready-to-use module for the simulation of N in the soil-plant system and interactions with farming practices, as well as ii) calibration datasets in which contrasting management and/or environmental conditions occur. Although some approaches are available for the simulation of soil N [70], crop N uptake, and partitioning/remobilization to plant organs [71], their use is partly limited by a general level of empiricism (i.e., most of them do not explicitly consider the dynamics of the soil microbes and fungi involved in the N soil cycle [64]). However, the simulation of non-limiting conditions for N availability is consistent with the information available from experiments performed by Parenti et al. [36], who demonstrated that very low fertilization rates are sufficient to guarantee potential production levels in the study area. Therefore, the N-fixing ability was not measured considering the complexity of the biological process that would have required a larger dataset, even though it may have played a role in increasing crop N availability [8]. The coupling of the crop model with a soil hydrological model was not necessary under the explored conditions because the combination of soil water retention capacity, mean seasonal cumulative precipitation (average = 224.5. ± 110.17 mm), and supplemental irrigation prevented any substantial water limitation to sunn hemp production at all experimental sites.

Even though the dataset used in the present model comes from variable field plot sizes, samples were carefully collected following the guidelines provided by Galezewski [72] to avoid overestimations and preserve plot representativeness (at least three border rows per side were excluded from each sampling area at the different locations). This would reduce yield overestimations from 23.5% to 2.3% in a 12 m^2 plot planted with legumes [72]. Significant biases in model accuracy were derived from the lack of consideration of plant-pest interactions in

Guadajira, where *Agriotes* spp. and *Spodoptera* spp. insects caused 10–20% yield losses due to early-season infestations [73]. Despite the development of specific and generic insect models [74], the use of integrated plant–insect approaches is still limited by two main bottlenecks: i) the population dynamics are often not explicitly simulated and ii) simulation of the impact on plants (e.g., leaf area or assimilation reduction) is mostly simplistic and requires observations on insect damage as input [64]. Another limitation of the study is the focus on a single variety. In this context, our perspective is to extend the application of SunnGro to Tropic Sunn, a highly productive long season variety, widely used in the subtropical climates of America [19]. SunnGro could be adapted to other cultivars via parameterization, given the availability of field experimental datasets, including dynamic measurements of crop phenology, LAI, BN, LN, and AGB. From this perspective, the ideal dataset would include a multi-year experiment consisting of the same varieties grown in contrasting agro-environmental conditions.

5. Conclusions

The new SunnGro model was proven capable of reproducing the canopy architecture and the aboveground biomass accumulation in sunn hemp under varying management practices and pedo-climatic conditions. In particular, the aboveground biomass was correctly simulated in Greece and Italy, especially at high sowing densities, while it was overestimated when low sowing rates and early harvest were adopted together in Italian conditions. A slight systematic overestimation of AGB occurred in Spain, but this was partly explained by early season pest attacks affecting one of the two experiments performed. The main innovation is the formulation of algorithms to simulate crop development and the evolution of leaf size/number and branch populations along the growing season, which achieved a balance between the accuracy of fit and model complexity. Compared to the available models, our approach provided more accurate predictions of aboveground biomass, which is crucial for the green energy sector and related activities, such as biogas and bioethanol production. The model can provide guidance to farmers in optimizing the sowing date and sowing density to maximize crop production in different European environments. It can also provide important indications for the potential biomass achievable using sunn hemp as a main or double crop under the explored conditions. Furthermore, compared to previous studies, SunnGro was demonstrated to be more accurate in predicting sunn hemp biomass yield when crop nitrogen and water requirements during the growing season were met. This study provides a decision support tool for private and public stakeholders in the agricultural sector. The modular approach at the core of BioMA allows for easy application of the model to other varieties, and fosters new model implementation, model reuse, and cross-domain model integration, as well as the link with georeferenced database at an optimal spatial resolution, with information on weather (current and future scenarios), soil, and management practices in the area of interest. The model is fully documented and released with a sample application showing how to use it (Software availability section). In this context, a user guide, illustrating the step-by-step procedure to launch the software, run the model, and create/modify the input and parameter files, drives the users in building customized simulation experiments according to their specific research/operational needs (Appendix E in supplementary material).

Acknowledgements

This work was supported by the European Union's Horizon 2020 Research and Innovation Programme (grant agreement 744821 – BECOOL project: https://www.becoolproject.eu/) and Italian Ministry of Agricultural, Food and Forestry Policies (MiPAAF) under the AGROENER project (D.D. n. 26329, April 1, 2016, http://agroener.crea.gov.it/).

Appendix A. Supplementary data

Supplementary data to this article can be found online at https://doi.org/10.1016/j.biombioe.2021.105975.

Software availability

BioMA component name: UniboCrea.SunnGro.

Developers: Fabrizio Ginaldi, Giovanni Cappelli, Andrea Parenti.

Availability and online documentation: UniboCrea.SunnGro is available as a Software Development Kit (SDK) on http://www.biomamodelling.org/Components/Components.aspx?node=30057. The SDK contains a help file comprising documentation for the algorithms and models, as well as a sample application illustrating how to use the component. A user guide explaining the step-by-step procedure to launch the software, run the model, and create/modify input and parameter files in order to build customized simulation experiments is given in Appendix E (supplementary material). UniboCrea.SunnGro is released as C# libraries compiled for. NET 4.5 platform.

References

[1] W. Zegada-Lizarazu, A. Monti, Energy crops in rotation, A review, Biomass Bioenergy. 35 (2011) 12–25, https://doi.org/10.1016/j.biombioe.2010.08.001.
[2] A.S. Voisin, J. Guéguen, C. Huyghe, M.H. Jeuffroy, M.B. Magrini, J.M. Meynard, C. Mougel, S. Pellerin, E. Pelzer, Legumes for feed, food, biomaterials and bioenergy in Europe: a review, Agron. Sustain. Dev. 34 (2014) 361–380, https://doi.org/10.1007/s13593-013-0189-y.
[3] W. Zegada-Lizarazu, H.W. Elbersen, S.L. Cosentino, A. Zatta, E. Alexopoulou, A. Monti, Agronomic aspects of future energy crops in Europe, Biofuels, Bioprod. Biorefining. 4 (2010) 674–691, https://doi.org/10.1002/bbb.242.
[4] K.A. Bybee-Finley, S.B. Mirsky, M.R. Ryan, Functional diversity in summer annual grass and legume intercrops in the northeastern United States, Crop Sci. 56 (2016) 2775–2790, https://doi.org/10.2135/cropsci2016.01.0046.
[5] J.L. Foster, J.P. Muir, J.R. Bow, E. Valencia, Biomass and nitrogen content of fifteen annual warm-season legumes grown in a semi-arid environment, Biomass Bioenergy 106 (2017) 38–42, https://doi.org/10.1016/j.biombioe.2017.08.016.
[6] R. Akanvou, L. Bastiaans, M. Kropff, J. Goudriaan, M. Becker, Characterization of growth, nitrogen accumulation and competitive ability of six tropical legumes for potential use in intercropping systems, J. Agron. Crop Sci. 187 (2001) 111–120, https://doi.org/10.1046/j.1439-037X.2001.00503.x.
[7] S.R. Kamireddy, J. Li, S. Abbina, M. Berti, M. Tucker, Y. Ji, Converting forage sorghum and sunn hemp into biofuels through dilute acid pretreatment, Ind. Crop. Prod. 49 (2013) 598–609, https://doi.org/10.1016/j.indcrop.2013.06.018.
[8] A.J. Ashworth, C.P. West, F.L. Allen, P.D. Keyser, S.A. Weiss, D.D. Tyler, A. M. Taylor, K.L. Warwick, K.P. Beamer, Biologically fixed nitrogen in legume intercropped systems: comparison of nitrogen-difference and nitrogen-15 enrichment techniques, Agron. J. 107 (2015) 2419–2430, https://doi.org/10.2134/agronj14.0639.
[9] S. Yoshida Mappaona, Mappaona, Growth and nitrogen fixation of Sesbania cannabina, Crotalaria juncea, and Cassia tora under the application of various forms of phosphorus, Soil Sci. Plant Nutr. 41 (1995) 613–619, https://doi.org/10.1080/00380768.1995.10419623.
[10] K.-H. Wang, B.S. Sipes, D.P. Schmitt, Crotalaria as a cover crop for nematode management: a review, Nematropica 32 (2002) 35–57.
[11] C.G. Cook, G.A. White, Crotalaria juncea: a potential multi-purpose fiber crop, in: J. Janick (Ed.), Prog. New Crop., 1996, pp. 389–394.
[12] P.P. Rotar, R.J. Joy, "Tropic Sun" Sunn Hemp, Crotalaria Juncea L., University of Hawaii, Hawaii, 1983.
[13] A.A. Abdul-baki, H.H. Bryan, G.M. Zinati, W. Klassen, M. Codallo, N. Heckert, Biomass yield and flower production in sunn hemp: effect of cutting the main stem, J. Veg. Crop Prod. 7 (2001) 83–104, https://doi.org/10.1300/j068v07n01_10.
[14] A.H. Cho, C.A. Chase, D.D. Treadwell, R.L. Koenig, J.B. Morris, J.P. Morales-Payan, Apical dominance and planting density effects on weed suppression by sunn hemp (Crotalaria juncea L.), Hortscience 50 (2015) 263–267.
[15] A. Parenti, W. Zegada-Lizarazu, A. Monti, Evaluation of sunn hemp productivity after wheat under no tillage conditions, in: 26th Eur. Biomass Conf. Exhib. Copenhagen, 2018, pp. 366–368.
[16] S.K. Paul, S. Chakraborty, Microwave-assisted ionic liquid-mediated rapid catalytic conversion of non-edible lignocellulosic sunn hemp fibres to biofuels, Bioresour. Technol. 253 (2018) 85–93, https://doi.org/10.1016/j.biortech.2018.01.010.
[17] M.F. Chagas, R.O. Bordonal, O. Cavalett, J.L.N. Carvalho, A. Bonomi, N.J. La Scala, Environmental and economic impacts of different sugarcane production systems in the ethanol biorefinery, Biofuels, Bioprod. Biorefining. 10 (2016) 89–106, https://doi.org/10.1002/bbb.
[18] K.B. Cantrell, P.J. Bauer, K.S. Ro, Utilization of summer legumes as bioenergy feedstocks, Biomass Bioenergy 34 (2010) 1961–1967, https://doi.org/10.1016/j.biombioe.2010.08.005.

[19] H.H. Schomberg, N.L. Martini, J.C. Diaz-Perez, S.C. Phatak, K.S. Balkcom, H. L. Bhardwaj, Potential for using sunn hemp as a source of biomass and nitrogen for the Piedmont and Coastal Plain Regions of the Southeastern USA, Agron. J. 99 (2007) 1448–1457, https://doi.org/10.2134/agronj2006.0294.

[20] Z. Mansoer, D.W. Reeves, C.W. Wood, Suitability of sunn hemp as an alternative late-summer legume cover crop, Soil Sci. Soc. Am. J. 61 (1997) 246–253, https://doi.org/10.2136/sssaj1997.03615995006100010034x.

[21] P.S. Teng, F. Penning de Vries, Editorial, Agric. Syst. 40 (1992) 1–3, https://doi.org/10.1016/0308-521x(92)90012-d.

[22] J.R. Porter, M.A. Semenov, Crop responses to climatic variation, Philos. Trans. R. Soc. B Biol. Sci. 360 (2005) 2021–2035, https://doi.org/10.1098/rstb.2005.1752.

[23] F. Ginaldi, S. Bajocco, S. Bregaglio, G. Cappelli, Spatializing crop models for sustainable agriculture, in: M. Farooq, M. Pisante (Eds.), Innov. Sustain. Agric., Springer, Cham, 2019, https://doi.org/10.1007/978-3-030-23169-9_20.

[24] K.J. Boote, M.I. Mínguez, F. Sau, Adapting the CROPGRO legume model to simulate growth of faba bean, Agron. J. 94 (2002) 743–756, https://doi.org/10.2134/agronj2002.7430.

[25] M.J. Robertson, P.S. Carberry, N.I. Huth, J.E. Turpin, M.E. Probert, P.L. Poulton, M. Bell, G.C. Wright, S.J. Yeates, R.B. Brinsmead, Simulation of growth and development of diverse legume species in APSIM, Aust. J. Agric. Res. 53 (2002) 429–446, https://doi.org/10.1071/AR01106.

[26] G.N. Falconnier, E.-P. Journet, L. Bedoussac, A. Vermue, F. Chlébowski, N. Beaudoin, E. Justes, Calibration and evaluation of the STICS soil-crop model for faba bean to explain variability in yield and N2 fixation, Eur. J. Agron. 104 (2019) 63–77, https://doi.org/10.1016/j.eja.2019.01.001.

[27] A. Soltani, K. Ghassemi-Golezani, F.R. Khooie, M. Moghaddam, A simple model for chickpea development, growth and yield, Field Crop. Res. 62 (1999) 213–224, https://doi.org/10.1016/j.fcr.2011.06.021.

[28] T.R. Sinclair, Water and nitrogen limitations in soybean grain production I. Model development, Field Crop. Res. 15 (1986) 125–141, https://doi.org/10.1016/0378-4290(86)90082-1.

[29] T.R. Sinclair, R.C. Muchow, M.M. Ludlow, G.J. Leach, R.J. Lawn, M.A. Foale, Field and model analysis of the effect of water deficits on carbon and nitrogen accumulation by soybean, cowpea and black gram, Field Crop. Res. 17 (1987) 121–140, https://doi.org/10.1016/0378-4290(87)90087-6.

[30] K.N. Le, J. Jeong, M.R. Reyes, M.K. Jha, P.W. Gassman, L. Doro, L. Hok, S. Boulakia, Evaluation of the performance of the EPIC model for yield and biomass simulation under conservation systems in Cambodia, Agric. Syst. 166 (2018) 90–100, https://doi.org/10.1016/j.agsy.2018.08.003.

[31] C.M. Bem, A.C. Filho, G.G. Chaves, J.A. Kleinpaul, R.V. Pezzini, A. Lavezo, Gompertz and logistic models to the productive traits of sunn hemp, J. Agric. Sci. 10 (2017) 225, https://doi.org/10.5539/jas.v10n1p225.

[32] C.M. Bem, A.C. Filho, G. Facco, D.E. Schabarum, D.L. Silveira, F.M. Simões, D. B. Uliana, Growth models for morphological traits of sunn hemp, Semina Ciências Agrárias 38 (2017) 2933–2944, https://doi.org/10.5433/1679-0359.2017v38n5p2933.

[33] T. Stella, C. Francone, S.S. Yamaç, E. Ceotto, V. Pagani, R. Pilu, R. Confalonieri, Reimplementation and reuse of the Canegro model: from sugarcane to giant reed, Comput. Electron. Agric. 113 (2015) 193–202, https://doi.org/10.1016/j.compag.2015.02.009.

[34] J.W. Jones, G. Hoogenboom, C.H. Porter, K.J. Boote, W.D. Batchelor, L.A. Hunt, P. W. Wilkens, U. Singh, A.J. Gijsman, J.T. Ritchie, The DSSAT Cropping System Model, 2003, https://doi.org/10.1016/S1161-0301(02)00107-7.

[35] A. Singels, M.R. Jones, M. Van Der Berg, DSSAT v4.5 Canegro sugarcane plant module. Scientific documentation, in: Int. Consort. Sugarcane Model., 2008, pp. 1–34.

[36] A. Parenti, W. Zegada-Lizarazu, A. Borghesi, A. Monti, Intercropping dedicated grass and legume crops for advanced biofuel production, in: 27th Eur. Biomass Conf. Exhib. Lisbon, 2019, pp. 105–107, https://doi.org/10.5071/27thEUBCE2019-1BO.9.5.

[37] M. Donatelli, I. Cerrani, D. Fanchini, D. Fumagalli, A.E. Rizzoli, Enhancing model reuse via component-centered modeling frameworks: the vision and example realizations, in: IEMSs 2012 - Manag. Resour. A Ltd. Planet Proc. 6th Bienn. Meet. Int. Environ. Model. Softw. Soc., 2012, pp. 1185–1192.

[38] C.O. Stockle, M. Donatelli, R. Nelson, CropSyst, a cropping systems simulation model, Eur. J. Agron. 18 (2003) 289–307, https://doi.org/10.1016/S1161-0301(02)00109-0.

[39] M.K. Van Ittersum, R. Rabbinge, Concepts in production ecology for analysis and quantification of agricultural input-output combinations, Field Crop. Res. 52 (1997) 197–208, https://doi.org/10.1016/S0378-4290(97)00037-3.

[40] M. Acutis, R. Confalonieri, Optimization algorithms for calibrating cropping systems simulation models. A case study with simplex-derived methods integrated in the WARM simulation environment, Ital. J. Agrometeorol. 3 (2006) 26–34.

[41] D.N. Moriasi, J.G. Arnold, M.W. Van Liew, R.L. Bingner, R.D. Harmel, T.L. Veith, Model evaluation guidelines for systematic quantification of accuracy in watershed simulations, Trans. ASABE (Am. Soc. Agric. Biol. Eng.) 50 (2007) 885–900, https://doi.org/10.13031/2013.23153.

[42] S.E. Jørgensen, L. Kamp-Nielsen, T. Christensen, J. Windolf-Nielsen, B. Westergaard, Validation of a prognosis based upon a eutrophication model, Ecol. Model. 32 (1986) 165–182.

[43] K. Loague, R.E. Green, Statistical and graphical methods for evaluating solute transport models : overview and application, J. Contam. Hydrol. 7 (1991) 51–73.

[44] J.E. Nash, J.V. Sutcliffe, River flow forecasting through conceptual models part I — a discussion of principles, J. Hydrol. 10 (1970) 282–290, https://doi.org/10.1016/0022-1694(70)90255-6.

[45] R. Taylor, Interpretation of the correlation coefficient: a basic review, J. Diagn. Med. Sonogr. 6 (1990) 35–39, https://doi.org/10.1177/875647939000600106.

[46] M.C. Peel, B.L. Finlayson, T.A. McMahon, Updated world map of the Köppen-Geiger climate classification, Hydrol. Earth Syst. Sci. 4 (2007) 439–473, https://doi.org/10.5194/hess-11-1633-2007.

[47] L.A. Monteiro, P.C. Sentelhas, G.U. Pedra, Assessment of NASA/POWER satellite-based weather system for Brazilian conditions and its impact on sugarcane yield simulation, Int. J. Climatol. 38 (2018) 1571–1581, https://doi.org/10.1002/joc.5282.

[48] M. Launay, M. Guérif, Ability for a model to predict crop production variability at the regional scale: an evaluation for sugar beet, Agronomie 23 (2003) 135–146, https://doi.org/10.1051/agro:2002078.

[49] M.A. Semenov, E.M. Barrow, LARS-WG, a Stochastic Weather Generator for Use in Climate Impact Studies. User Manual, Rothamsted Res. Harpenden, Hertfordshire, AL5 2JQ, UK, 2002, p. 27.

[50] C.O. Stöckle, G.S. Campbell, R. Nelson, ClimGen Manual, Biological Systems Engineering Department, Washington State University, Pullman, WA, 1999, p. 28.

[51] I.A. Ciampitti, W.T. Schapaugh, D. Shoup, S. Duncan, D.R. Diaz, D. Peterson, D. H. Rogers, J. Whitworth, H. Schwarting, D. Jardine, J. Harner, M. Taylor, D. M. O'Brien, J. O'Neil, A. Sharda, L. Haag, Soybean Production Handbook, 2016.

[52] H. Wickham, Ggplot2: Elegant Graphics for Data Analysis, Springer-Verlag, New York, 2009.

[53] A. Qi, T.R. Wheeler, J.D.H. Keatinge, R.H. Ellis, R.J. Summerfield, P.Q. Craufurd, Modelling the effects of temperature on the rates of seedling emergence and leaf appearance in legume cover crops, Exp. Agric. 35 (1999) 327–344, https://doi.org/10.1017/S0014479799003099.

[54] P.Q. Craufurd, R.H. Ellis, R.R.J. Summerfield, L. Menin, Development in cowpea (Vigna unguiculata). I. The influence of temperature on seed germination and seedling emergence, Exp. Agric. 32 (1996) 1–12, https://doi.org/10.1017/S0014479700025801.

[55] P.Q. Craufurd, R.J. Summerfield, R.H. Ellis, E.H. Roberts, Photoperiod, temperature, and the growth and the development of cowpea, in: B.B. Singh, D. R. Mohan Raj, K.E. Dashiell, L.E.N. Jackai (Eds.), Adv. Cowpea Res., IITA and JIRCAS, 1997, pp. 75–86. Ibadan, Nigeria.

[56] H.D.J. van Heemst, Plant Data Values Required for Simple Crop Growth Simulation Models: Review and Bibliography, 1988. Available at: https://edepot.wur.nl/218353.

[57] E.R. Boons-Prins, G.H. de Koning, C.A. van Diepen, F.W.T. Penning de Vries, Crop-specific Simulation Parameters for Yield Forecasting across the European Community, 1993.

[58] P. Dart, F. Mercer, The effect of growth temperature, level of ammonium nitrate, and light intensity on the growth and nodulation of cowpea (Vigna sinensis endl. ex hassk.), Aust. J. Agric. Res. 16 (1965) 321, https://doi.org/10.1071/AR9650321.

[59] J. Lecoeur, B. Ney, Change with time in potential radiation-use efficiency in field pea, Eur. J. Agron. 19 (2003) 91–105, https://doi.org/10.1016/S1161-0301(02)00019-9.

[60] M. Van Oijen, A. Schapendonk, M. Höglind, On the relative magnitudes of photosynthesis, respiration, growth and carbon storage in vegetation, Ann. Bot. 105 (2010) 793–797, https://doi.org/10.1093/aob/mcq039.

[61] E.J. Littleton, M.D. Dennett, J. Elston, J.L. Monteith, The growth and development of cowpeas (Vigna unguiculata) under tropical field conditions: 1. Leaf area, J. Agric. Sci. 93 (1979) 291–307, https://doi.org/10.1017/S0021859600037977.

[62] T.S. Moroke, R.C. Schwartz, K.W. Brown, A.S.R. Juo, Soil water depletion and root distribution of three dryland crops, Soil Sci. Soc. Am. J. 69 (2005) 197–205, https://doi.org/10.2136/sssaj2005.0197.

[63] R.G. Allen, L.S. Pereira, D. Raes, M. Smith, Crop evapotranspiration. Guidelines for computing crop water requirements, FAO Irrigation and drainage paper 56, FAO 300 (9) (1998) D05109. Available at: http://www.fao.org/3/X0490E/x0490e00.htm.

[64] M. Donatelli, R. Confalonieri, Biophysical models for cropping system simulation, in: G. Flichman (Ed.), Bio-Economic Model. Appl. To Agric. Syst., Bio-Econom, Springer, 2011, pp. 59–87.

[65] H.D. Adams, A.P. Williams, C. Xu, S.A. Rauscher, X. Jiang, N.G. McDowell, Empirical and process-based approaches to climate-induced forest mortality models, Front. Plant Sci. 4 (2013) 1–5, https://doi.org/10.3389/fpls.2013.00438.

[66] G. Cappelli, R. Confalonieri, M. Romani, S. Feccia, M.A. Pagani, C. Cappa, S. Bocchi, S. Bregaglio, Boundaries and perspectives from a multi-model study on rice grain quality in Northern Italy, Field Crop. Res. 215 (2018) 140–148, https://doi.org/10.1016/j.fcr.2017.10.014.

[67] G. Cappelli, F. Zanetti, F. Ginaldi, D. Righini, A. Monti, S. Bregaglio, Development of a process-based simulation model of camelina seed and oil production: a case study in Northern Italy, Ind. Crop. Prod. 134 (2019) 234–243, https://doi.org/10.1016/j.indcrop.2019.03.046.

[68] C. Gilardelli, T. Stella, N. Frasso, G. Cappelli, S. Bregaglio, M.E. Chiodini, B. Scaglia, R. Confalonieri, Wofost-Gtc, A new model for the simulation of winter rapeseed production and oil quality, Field Crop. Res. 197 (2016) 125–132, https://doi.org/10.1016/j.fcr.2016.07.013.

[69] K.T. Zeleke, D.J. Luckett, R.B. Cowley, The influence of soil water conditions on canola yields and production in Southern Australia, Agric. Water Manag. 144 (2014) 20–32, https://doi.org/10.1016/j.agwat.2014.05.016.

[70] D.K. Benbi, J. Richter, A critical review of some approaches to modelling nitrogen mineralization, Biol. Fertil. Soils 35 (2002) 168–183, https://doi.org/10.1007/s00374-002-0456-6.

[71] L. Ma, T. Bruulsema, L.R. Ahuja, Quantifying and Understanding Plant Nitrogen Uptake for Systems Modeling, CRC Press, 2008, https://doi.org/10.1201/9781420052978.

[72] L. Galezewski, M. Piekarczyk, I. Jaskulska, P. Wasilewski, Border effects in the growth of chosen cultivated plant species, Acta Sci. Pol. Agric. 12 (2013) 3–12.
[73] C.M. Sastre, C.S. Ciria, P. Ciria, J. Carrasco, WP1: biomass production and feedstock diversification for advanced biofuels, 13-14 June 2018. Borgo San Lorenzo (Italy), in: Oral Presentation at BECOOL 3rd Technical Meeting, 2018. Available at: https://www.becoolproject.eu/login/?redirect_to=%2Fprivate%2F.
[74] M. Donatelli, R.D. Magarey, S. Bregaglio, L. Willocquet, J.P.M. Whish, S. Savary, Modelling the impacts of pests and diseases on agricultural systems, Agric. Syst. 155 (2017) 213–224, https://doi.org/10.1016/j.agsy.2017.01.019.